Dail and Hammar's Pulmonary Pathology

Third Edition

Dail and Hammar's Pulmonary Pathology

Volume I: Nonneoplastic Lung Disease

Third Edition

Editor

Joseph F. Tomashefski, Jr., MD
Professor, Department of Pathology, Case Western Reserve University School of Medicine; Chairman, Department of Pathology, MetroHealth Medical Center, Cleveland, Ohio, USA

Associate Editors

Philip T. Cagle, MD
Professor, Department of Pathology, Weill Medical College of Cornell University, New York, New York; Director, Pulmonary Pathology, Department of Pathology, The Methodist Hospital, Houston, Texas, USA

Carol F. Farver, MD
Director, Pulmonary Pathology, Department of Anatomic Pathology, The Cleveland Clinic Foundation, Cleveland, Ohio, USA

Armando E. Fraire, MD
Professor, Department of Pathology, University of Massachusetts Medical School, Worcester, Massachusetts, USA

Springer

Editor:
Joseph F. Tomashefski, Jr., MD
Professor, Department of Pathology, Case Western Reserve University School of Medicine; Chairman, Department of Pathology, MetroHealth Medical Center, Cleveland, OH, USA

Associate Editors:
Philip T. Cagle, MD
Professor, Department of Pathology, Weill Medical College of Cornell University, New York, NY; Director, Pulmonary Pathology, Department of Pathology, The Methodist Hospital, Houston, TX, USA

Carol F. Farver, MD
Director, Pulmonary Pathology, Department of Anatomic Pathology, The Cleveland Clinic Foundation, Cleveland, OH, USA

Armando E. Fraire, MD
Professor, Department of Pathology, University of Massachusetts Medical School, Worcester, MA, USA

Library of Congress Control Number: 2007920839

Volume I ISBN: 978-0-387-98395-0 e-ISBN: 978-0-387-68792-6
DOI: 10.1007/978-0-387-68792-6

Set ISBN: 978-0-387-72139-2

Printed on acid-free paper.

9 8 7 6 5 4 3 2 1

springer.com

To
David H. Dail
Samuel P. Hammar

For their many contributions to pulmonary pathology, and for their conceptual and sustaining vision of this textbook

Joseph F. Tomashefski, Jr.
Philip T. Cagle
Carol F. Farver
Armando E. Fraire

To my dear wife, Cathy, and our children, Amy, Cary, David, Jessica, and Sarah

Joseph F. Tomashefski, Jr.

To my wife, Kirsten

Philip T. Cagle

To the memory of my parents, Albert and Gladys Farver

Carol F. Farver

In memory of Dr. S. Donald Greenberg, dear friend, respected colleague, and superb teacher

Armando E. Fraire

Preface

It is with a great sense of good fortune, humility, and responsibility that we, the editors, have undertaken the task of updating Dail and Hammar's *Pulmonary Pathology*, one of the great modern textbooks not only in the field of lung pathology but also in the wider arena of general pathology as well. Following the publication of its first edition, "Dail and Hammar" rapidly became the standard against which subsequent textbooks of lung pathology were measured.

First published in 1987, *Pulmonary Pathology* provided an alternative to Herbert Spencer's time-honored text, *Pathology of the Lung* which, in its fourth edition at that time, was the reigning tome on the pathology of the respiratory system. The first edition of "Dail and Hammar" was in part dedicated to Dr. Spencer, who graciously penned the foreword for that text. The first edition was also dedicated to Averill Liebow, one of the giants of pulmonary pathology, under whom Dr. Dail had served and been mentored as a fellow. Dr. Liebow's influence was notable in the first two editions, and has continued in this edition in the revised classifications and current understanding of interstitial pneumonias and lung tumors, subjects in which Dr. Liebow played such a defining role. Several of Dr. Liebow's timeless original illustrations continue to grace the pages of the third edition.

In the 13 years since the second edition there have been astounding advances in medicine and pathology. The current edition has been revised and updated to reflect these advances. As much as possible, however, we have striven to remain true to Drs. Dail and Hammar's original goals, "to present the reader with an authoritative yet readable text which hopefully answers questions that might arise in facing problem cases and to offer the reader appropriate review of particular areas within the field of pulmonary pathology." In the face of wide-reaching revisions our intent has been to maintain the unique character of *Pulmonary Pathology*, and retain continuity with previous editions. Dr. Dail and Dr. Hammar have continued to play a major role in the present text, together contributing as author or coauthor to approximately one fourth of the chapters. Nine other chapters have been updated by contributors who were also featured in the second edition. Many, if not the majority, of the illustrations in the text represent the color counterparts of previous black-and-white figures. Electron microscopy, which was emphasized in the previous two editions, continues to have a presence in the third, mainly in the volume on neoplasia, and lays the foundation for a deep understanding of the histological appearances of tumors.

The changes in the current edition, however, are significant. The previous sizable single volume text has been divided into two volumes, covering neoplastic and non-neoplastic lung diseases, to afford the reader more ready access and less strenuous effort when referencing the sections of interest. Entirely new chapters have been added on the pathology of small airways disease (Chapter 25), forensic lung pathology (Chapter 31), molecular genetics of lung and pleural neoplasms (Chapter 33), and preinvasive (neoplastic) disease (Chapter 34). The topics formerly included in the second edition chapters on AIDS and tobacco-related injury have been

dispersed in the third edition, mainly throughout the sections on lung infections and lung cancer, respectively. Similarly the monumental chapters on common and uncommon lung tumors in the previous editions have been divided into seven smaller topical units housed in the second volume. Over 90 percent of the illustrations in the current edition are now presented in vivid color.

Pulmonary Pathology was one of the first pathology textbooks to emphasize the burgeoning field of immunohistochemistry and its application to diagnostic pathology, and the current edition continues to expound on the important diagnostic role of immunohistochemical stains. In this edition, however, we also embrace the molecular age with updated information on molecular pathology. In addition to extensive references to molecular aspects of lung disease, which are integrated within each of the individual chapters, the new edition includes two chapters (Chapters 33 and 34) devoted almost exclusively to molecular pathology. Chapter 33 (Molecular Genetics of Lung and Pleural Neoplasms) is essentially a text-within-a-text, serving as a compendium of information on the molecular pathology of lung tumors as well as a primer on basic molecular pathology for the uninitiated or molecularly challenged pathologist.

Within reason and to the best of our ability we have tried to maintain the reputation of *Pulmonary Pathology* as a comprehensive textbook that not only serves as a diagnostic guide to the "labyrinths of the lung," but also enables the reader to explore the etiology and pathogenesis of lung diseases. The references, both classical and modern, have been greatly increased and, as of the time that the book went to press, are relatively current. The present edition also recognizes the growing importance of electronic information sources. Relevant Internet Web sites have been included among the chapter references, and Chapter 22 on pulmonary drug toxicity is essentially constructed around Web-based resources.

There are numerous individuals to whom we owe a debt of gratitude. Most importantly, we thank the many authors who gave of their time and talent, without

Figure 1. Members of the editorial board with Drs. Dail and Hammar. (From left to right: Carol F. Farver, Philip T. Cagle, David H. Dail, Samuel P. Hammar, Armando E. Fraire, and Joseph F. Tomashefski, Jr.)

financial compensation, to contribute to this book. Their expertise and dedication represent the soul of the work. We also appreciate their patience and understanding as both authors and editors faced the stressful implications of rapidly approaching (and receding) publication deadlines. We recognize and are especially thankful for the wonderful pulmonary pathologists under whom we have trained, who taught us the trade and served as our role models: Dr. S. Donald Greenberg (Drs. Cagle and Fraire); Dr. William Thurlbeck (Dr. Cagle); Drs. Jerome Kleinerman, John D. Reid, Merle Legg, and Lynne Reid (Dr. Tomashefski); and Drs. John Godleski and Les Kobzik (Dr. Farver). Finally, we are grateful to the Springer publishing firm, especially to our executive editor, Melissa Ramondetta and her editorial assistant, Dianne Wuori. A special thanks goes to our developmental editor, Stephanie Sakson, who kept us on track throughout the process, surmounting the hurdles of copyright permits, and the inexorable correlation of images, references, and text.

From the editors' perspective our labors now are ended (for a while at least). We leave it to you, the reader, to evaluate this text. We welcome your comments, positive or negative, which may help to direct future editions.

Joseph F. Tomashefski, Jr., MD
Philip T. Cagle, MD
Carol F. Farver, MD
Armando E. Fraire, MD

Contents

Volume I: Nonneoplastic Lung Disease

Volume II: Neoplastic Lung Disease

Contributors

Patrick A. Adegboyega, MD
Department of Pathology, University of Texas Medical Branch, Galveston, TX 77555, USA

Timothy C. Allen, MD, JD
Chairman, Department of Pathology, University of Texas Health Center at Tyler, Tyler, TX 75708, USA

Roberto Barrios, MD
Attending Pathologist, Department of Pathology, The Methodist Hospital, Houston, TX 77030, USA

Mary Beth Beasley, MD
Department of Pathology, Providence Portland Medical Center, Portland, OR 97210, USA

Kelly J. Butnor, MD
Assistant Professor, Department of Pathology, University of Vermont/Fletcher Allen Health Care, Burlington, VT 05401, USA

Philip T. Cagle, MD
Professor, Department of Pathology, Weill Medical College of Cornell University, New York; *and* Director, Pulmonary Pathology, Department of Pathology, The Methodist Hospital, Houston, TX 77030, USA

Thomas V. Colby, MD
Consultant in Pathology, Mayo Clinic Scottsdale, Scottsdale, AZ 85259, USA

Carlyne D. Cool, MD
Department of Pathology, University of Colorado Health Sciences Center, Denver, CO 80262, USA

David H. Dail, MD
Staff Pathologist, Department of Pathology, Virginia Mason Medical Center, Seattle, WA 98101, USA

Louis P. Dehner, MD
Professor and Director, Division of Anatomic Pathology, Washington University School of Medicine, St. Louis, MO 63122, USA

Ronald F. Dodson
ERI Consulting, Inc., 2026 Republic Drive, Ste A, Tyler, TX 75701, USA

Carol F. Farver, MD
Director, Pulmonary Pathology, Department of Anatomic Pathology, The Cleveland Clinic Foundation, Cleveland, OH 44195, USA

Douglas B. Flieder, MD
Chief of Surgical Pathology, Fox Chase Cancer Center, Philadelphia, PA 19111, USA

Armando E. Fraire, MD
Professor, Department of Pathology, University of Massachusetts Medical School, Worcester, MA 01655, USA

Anthony A. Gal, MD
Professor, Department of Pathology and Laboratory Medicine, Emory University Hospital, Atlanta, GA 30322, USA

Michael A. Graham, MD
Professor, St. Louis University School of Medicine; *and* Chief Medical Examiner, City of St. Louis, Division of Forensic and Environmental Pathology, St. Louis, MO 63104, USA

Steve D. Groshong, MD, PhD
Instructor, Department of Pathology, University of Colorado Health Sciences Center, Denver, CO 80262, USA

Donald G. Guinee, Jr., MD
Pathologist, Department of Pathology, Virginia Mason Medical Center, Seattle, WA 98111, USA

Samuel P. Hammar, MD
Harrison Medical Center, Pathology Associates of Kitsap County, Bremerton, WA 98310, USA

Abida K. Haque, MD
Medical Director, Department of Pathology, San Jacinto Methodist Hospital, Baytown, TX 77521, USA

Philip Hasleton, MD, FRCPath
Professor, Department of Histopathology, Clinical Sciences Block, Manchester Royal Infirmary, Manchester M13 9WL, UK

Douglas W. Henderson, MB, BS, FRCPA, FRCPath, FHKCPath (Hon)
Professor and Senior Consultant, Departments of Pathology and Anatomical Pathology, Flinders Medical Centre, Bedford Park 5042, Adelaide, South Australia

Elise R. Hoff, MD
Department of Pathology, University of Pittsburgh Medical Center—Presbyterian, Pittsburgh, PA 15213, USA

Aliya N. Husain, MB, BS
Professor, Department of Pathology, University of Chicago, Chicago, IL 60637, USA

Jaishree Jagirdar, MD
Department of Pathology, University of Texas Health Science Center at San Antonio, San Antonio, TX 78284, USA

Keith M. Kerr, BSc(Hons) MB ChB FRCPath
Consultant, Pathologist and Clinical Senior Lecturer, Department of Pathology, Aberdeen Royal Infirmary and Aberdeen University School of Medicine, Foresterhill, Aberdeen, AB25 2ZD, UK

Andras Khoor, MD
Department of Pathology, Mayo Clinic Jacksonville, Jacksonville, FL 32224, USA

Sonja Klebe, MD, PhD, FRCPA
Senior Lecturer in Anatomical Pathology, Flinders University and Consultant in Anatomical Pathology, Flinders Medical Centre, Bedford Park 5042, Adelaide, South Australia

Les Kobzik, MD
Associate Professor, Department of Environmental Health, Harvard School of Public Health, Boston, MA 02115, USA

P. Rocco LaSala, MD
Fellow, Medical Microbiology, Department of Pathology, University of Texas Medical Branch, Galveston, TX 77555, USA

Kevin O. Leslie, MD
Consultant and Professor, Mayo Clinic College of Medicine, Rochester, MN; *and* Department of Laboratory Medicine and Pathology, Mayo Clinic Scottsdale, Scottsdale, AZ 85259, USA

Aileen M. Marty, MD, FACP
Senior Scientific Advisor to the Undersecretary for Science and Technology Directorate, DHS, Department of Homeland Security, National Defense University, North Bethesda, MD 20852, USA

Michael R. McGinnis, PhD
Professor, Department of Pathology, University of Texas Medical Branch, Galveston, TX 77555, USA

William George Morice, MD, PhD
Consultant, Associate Professor of Medicine, Departments of Hematopathology and Anatomic Pathology, Mayo Clinic, Mayo Medical School, Rochester, MN 55905, USA

Andrew G. Nicholson, FRCPath DM
Professor of Respiratory Pathology, National Heart and Lung Institute Division of Imperial College School of Medicine and Consultant Histopathologist, Royal Brompton Hospital, Department of Histopathology, Sydney Street, London SW3 6NP, UK

N. Paul Ohori, MD
Medical Director of Cytopathology, Department of Pathology, University of Pittsburgh Medical Center—Presbyterian, Pittsburgh, PA 15213, USA

Christopher D. Paddock, MD, MS, MPHTM
Staff Pathologist, Department of Infectious Disease Pathology Activity, Centers for Disease Control and Prevention, Atlanta, GA 30333, USA

Helmut H. Popper, MD, Prof. Pathol.
Department of Pathology, University of Graz, Auenbruggerplatz 25, Graz A-8036, Austria

Gary W. Procop, MD, MS
Section Head, Clinical Microbiology, Division of Pathology and Laboratory Medicine, The Cleveland Clinic Foundation, 9500 Euclid Avenue, Cleveland, OH 44195

Victor L. Roggli, MD
Department of Pathology, Duke University and Durham VA Medical Centers, Durham, NC 27705, USA

Thomas A. Sporn, MD
Department of Pathology, Duke University and Durham VA Medical Centers, Durham, NC 27710, USA

J. Thomas Stocker, MD
Professor of Pathology, Uniformed Services University of the Health Sciences, 4301 Jones Bridge Road, Bethesda, MD 20814

Joseph F. Tomashefski, Jr., MD
Professor, Department of Pathology Case Western Reserve University School of Medicine; Chairman, Department of Pathology MetroHealth Medical Center Cleveland, OH 44109, USA

William D. Travis, MD
Attending Thoracic Pathologist, Department of Pathology, Memorial Sloan Kettering Cancer Center, New York, NY 10021, USA

David H. Walker, MD
Department of Pathology, University of Texas Medical Branch, Galveston, TX 77555, USA

Washington C. Winn, Jr., MD
Fletcher Allen Health Care, University of Vermont College of Medicine, Burlington, VT 05482, USA

Sherif R. Zaki, MD, PhD
Chief, Infectious Disease Pathology Activity, Department of Infectious Disease Pathology Activity, Centers for Disease Control and Prevention, Atlanta, GA 30333, USA

Dani S. Zander, MD
Professor and Chair, Department of Pathology, Penn State Milton S. Hershey Medical Center, Hershey, PA 17033, USA

1
Tissue Procurement, Sampling, and Preparation

Joseph F. Tomashefski, Jr.

The approach to the morphological diagnosis of lung disease varies with the type of tissue sample submitted and the associated clinical setting. Tissue samples can be roughly grouped into three major categories: (1) small biopsy specimens; (2) surgical lung biopsy specimens; and (3) large specimens including those obtained by lobectomy, pneumonectomy, or autopsy. The clinical situation usually dictates the manner of tissue procurement. For example, a central endobronchial lesion is approached via endoscopic biopsy under direct visualization, whereas a peripheral or perihilar mass is better accessed by a computed tomography (CT)-guided transthoracic or an endoscopic transbronchial needle biopsy, respectively. Transbronchial forceps lung biopsy is often the initial procedure in stable immunocompetent patients with interstitial lung disease, but an open lung biopsy or a biopsy obtained by video-assisted thoracoscopic surgery (VATS) may be the preferred diagnostic modality in immunosuppressed patients with rapidly evolving pulmonary infiltrates. Regardless of the means of tissue procurement, a review of the clinical and radiological data by the pathologist is essential for appropriate tissue handling and interpretation. High-resolution CT scan has become the modern pathologist's "gross specimen" in the assessment of lung biopsy samples.[1] In some areas of lung pathology, such as the idiopathic interstitial pneumonias, the final diagnosis is sometimes an integration of histological and radiological findings (see Chapter 19).

This chapter reviews the standard techniques used to sample lung tissue, and the assessment and handling of lung specimens at the dissecting bench and in the histology laboratory. Special emphasis is placed on the limitations of sampling techniques, diagnostic yield, and the pitfalls of interpretation associated with different modalities of lung biopsy. The handling of lung tissue at autopsy is also addressed in this chapter and is further discussed in the chapter on forensic pathology (Chapter 31). At the end of this chapter an overview of special techniques applied to the study of lung pathology is provided. Cytological sampling is discussed in Chapter 45 and pleural biopsy techniques are reviewed in Chapter 30.

Small Biopsy Specimens

The key to success in diagnostic lung pathology is to maximize the information that can be obtained from the tissue sample provided. A tenacious, yet judicious, end-in-mind approach, which appropriately conserves and allocates tissue for essential diagnostic testing is paramount. Howard Andersen, a pioneer in the development of the transbronchoscopic lung biopsy, recognized and summarized the importance of this general philosophy when he stated, "It is necessary not only to have satisfactory biopsy specimens, but it is particularly important to have an interested and experienced pathologist who is willing to glean everything possible from these tiny pieces of tissue. If such a person is not available, the endoscopist need not attempt transbronchoscopic lung biopsies."[2] On the other hand, it is equally important that the pathologist understand the limitations of these small specimens and realize when a nonspecific, descriptive diagnosis is appropriate. Even a nonspecific diagnosis is important in patient management, as it will often result in clinical reconsideration, exclude certain diagnostic possibilities, and lead to additional diagnostic testing.[3]

The handling of most small tissue samples, including those obtained by endoscopic forceps biopsy, or by transbronchial or transthoracic needle biopsy, is similar. A standard approach includes fixation followed by serial step-sectioning and staining of selected sections with hematoxylin and eosin (H&E), preserving the interval unstained sections on adhesive slides for subsequent histochemical or immunohistochemical staining. In our laboratory we routinely set five or six serial sections per slide and initially stain slides 1, 4, and 7. The tissue remaining in the paraffin block can be utilized as needed. For very minute specimens additional unstained sections may be

cut initially. Close communication between the pathologist and the histotechnologist is critical in preparing or selecting levels that are most likely to give a positive staining result. Tissue or fluids for microbiological culture should be obtained separately and submitted directly to the microbiology laboratory from the procedure room. When indicated, tissue for special studies such as direct immunofluorescence (DIF) microscopy or electron microscopy (EM) is submitted separately either as fresh tissue or in the appropriate fixative, but processing should be withheld until after the initial H&E sections have been reviewed to ensure that there is satisfactory tissue for histological diagnosis.

A variety of fixatives, including formaldehyde and nonformaldehyde preservatives, are available for routine tissue fixation. The author uses 10% neutral buffered formalin as a general fixative. Most immunohistochemical procedures can now be performed on formalin-fixed tissue without the need for fresh-frozen tissue or other special preservatives, provided that appropriate antigen retrieval methods are available to recover those antigens that are diminished or modified.[4] However, for suspected lymphoproliferative lesions, especially in large tissue samples, at least one piece of tissue is fixed in B-5 fixative. When EM studies are necessary, a fresh tissue sample is either submitted directly or minced into cubic-millimeter-sized fragments and placed in glutaraldehyde. Other EM fixatives such as Karnovsky's solution are also excellent.

A basic armamentarium of special stains should be available to the lung pathologist. The stains most frequently used are those for microorganisms (tissue gram stain [Brown-Brenn or Brown-Hopps], Gomori methenamine silver stain for fungi, and Ziehl-Neelsen stain for acid-fast bacilli), for connective tissue (elastic van Gieson or Movat pentachrome, and Masson trichrome), and for iron (Perls or Prussian blue), in addition to histochemical (e.g., periodic acid-Schiff and mucicarmine) and immunohistochemical stains to delineate the components of neoplasms. Other special stains are utilized as needed. Polarizing filters should also be used routinely to search for crystals and other birefringent material in the evaluation of nonneoplastic lung disease. The application and interpretation of special stains, including fluorescent, immunofluorescent and immunohistochemical techniques, in the morphological detection of microorganisms are reviewed in the chapters on infectious diseases (Chapters 8 to 14). Immunohistochemical and histochemical stains used in the classification of neoplasms are extensively discussed in volume 2, which is devoted to neoplastic lung disease.

Bronchoscopic Biopsy

The rigid bronchoscope, traditionally utilized by surgeons, currently serves a limited function mainly for the extraction of tracheobronchial foreign bodies, control of massive hemoptysis, placement of bronchial stents, and laser ablation surgery.[5–7]

Flexible fiberoptic bronchoscopy (FFB), introduced by Ikeda in 1967, has largely replaced rigid bronchoscopy as the standard method for visualization of the bronchial tree and biopsy of bronchi and surrounding parenchyma (Fig. 1.1).[5,8–10] Compared to the rigid bronchoscope, which provides visual access only to the orifices of segmental bronchi, the fiberoptic bronchoscope can reach to the origins of about 56% of sixth-order bronchi and physically enter approximately 38% of fifth-order bronchi.[11] Flexible fiberoptic bronchoscopy is particularly advantageous in navigating the angulated bronchial divisions of the upper lobe. Hinged cup-shaped forceps with a cutting edge or serrated alligator forceps grasp tissue fragments on the order of 1 to 3 mm in maximal dimension (Fig. 1.1).[11,12] Endobronchial biopsy is the preferred method for sampling intrabronchial lesions.[9] Three or four tissue samples are recommended to achieve a diagnostic success rate of nearly 100%.[13–15]

Transbronchial biopsy (TBB) provides samples of pulmonary parenchyma or peripheral mass lesions by

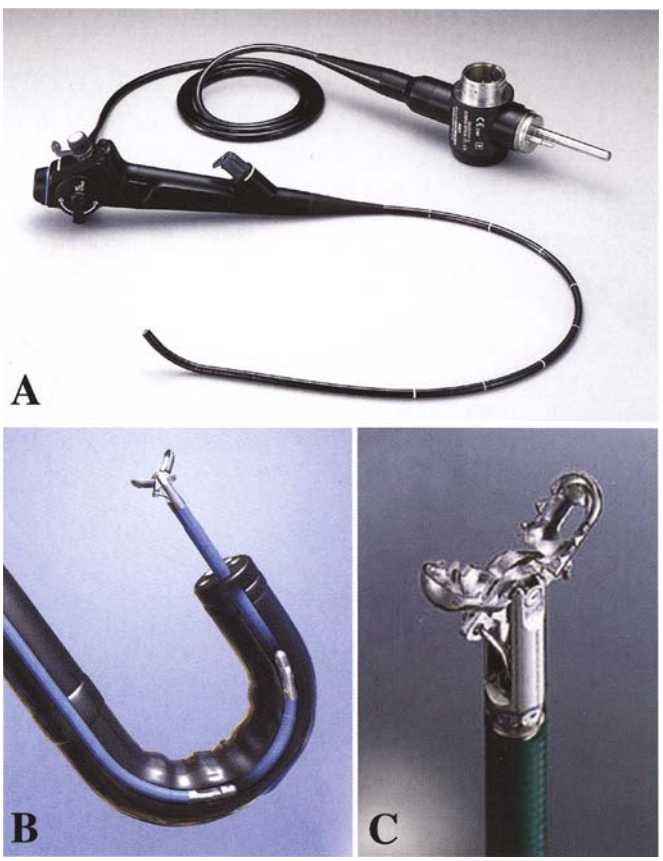

FIGURE 1.1. **A.** Adult flexible fiberoptic bronchoscope. **B.** Extension of biopsy forceps through endoscope channel. **C.** Magnified image of serrated alligator jaw biopsy forceps. (Courtesy of Olympus America Inc., Melville, NY.)

extending the biopsy forceps, often under fluoroscopic guidance, beyond the visual range of the bronchoscope.[9,10] Transbronchial biopsy is frequently done in concert with bronchial washing or bronchial brushing (BB) to obtain cytologic specimens (see Chapter 45). Transbronchial biopsy is a relatively safe procedure with a low mortality rate (approximately 0.1% to 0.2%), the major complications being pneumothorax (3% to 5%) and hemorrhage (9% in routine cases).[12,16,17] The risk of significant hemorrhage is increased in patients on mechanical ventilation or in patients with bleeding disorders, immunosuppression, pulmonary hypertension, or uremia.[10,12,16]

Diagnostic Yield of Transbronchial Biopsy

The diagnostic yield of TBB is influenced by the patient population, underlying diseases, and whether or not nonspecific chronic inflammation and fibrosis is considered as a specific histologic entity.[3] For peripheral mass lesions the diagnostic yield by TBB ranges from 30% to 80% (average, approximately 50%).[12] The diagnostic yield for malignant nodules (63%) is greater than for benign lesions (38%), and the yield for central neoplasms exceeds that for peripheral tumors.[15,18] The diagnostic success rate also increases with the size of the lesion and with the number of samples obtained.[15,19–21] In one study, 75% of peripheral tumors were diagnosed with a six-sample protocol.[15] The addition of bronchial washing and brushing cytology further increases the diagnostic yield.[15,22,23]

The diagnostic yield of TBB for localized or diffuse infiltrates is limited not only by inconsistent tissue sampling of irregularly distributed lesions but also by the nonspecific features of chronic inflammation and fibrosis that characterize many pulmonary disorders.[24] Specific histologic diagnoses, however, can be frequently achieved for selected diseases such as infections, sarcoidosis, and malignancy (including lymphangitis carcinomatosa), and occasionally determined for diseases such as pulmonary Langerhans' cell granulomatosis, Wegener's granulomatosis, pulmonary alveolar proteinosis, amyloidosis, and lymphangioleiomyomatosis.[1,12,25–32] In other conditions, including collagen vascular diseases, eosinophilic pneumonia, drug reactions (e.g., amiodarone toxicity), and hypersensitivity pneumonitis, nonspecific histologic features in conjunction with a strong clinical-pathologic correlation may be sufficient to establish a clinical-pathologic diagnosis. Ancillary studies such as DIF, EM, or microbiologic cultures may additionally provide a specific diagnosis in some cases with nonspecific histologic features. However, for idiopathic interstitial pneumonias, lymphoproliferative disorders and pneumoconioses, the findings on TBB are generally inadequate to determine a definitive diagnosis.[1,33,34]

A reasonable diagnostic yield of TBB in nonimmunocompromised patients with diffuse lung disease is around 30% to 40% if nonspecific diagnoses are excluded.[2,3,21,33–40] Transbronchial biopsy samples are inadequate or consist of normal lung tissue in up to 21% of cases.[2,3,40] The clinical implication of a nonspecific diagnosis on TBB was evaluated by Wilson and colleagues,[41] who concluded that patients with a peripheral mass lesion were often subsequently found to have cancer, whereas nonimmunocompromised patients with localized or diffuse infiltrates frequently had a benign clinical course that did not warrant a follow-up open lung biopsy.

The diagnostic yield of FFB (including TBB, cultures, and cytologic evaluation of bronchial brushings and washings) in immunosuppressed patients without acquired immune deficiency syndrome (AIDS) ranges from 52% to 88% (most series include nonspecific interstitial pneumonitis in the diagnostic category).[42–48] Flexible fiberoptic bronchoscopy is more likely to establish the diagnosis when the lung infiltrate is due to an infectious agent than to a noninfectious process.[48–50] A greater diagnostic yield has also been reported in diffuse versus localized radiographic infiltrates.[42,51] However, neither Jain and colleagues[49] nor Matthay and colleagues[43] found a difference in diagnostic yield relative to the radiographic distribution of disease. Transbronchial biopsy alone provides a specific histologic diagnosis in about 38% of immunocompromised patients.[49] The combination of TBB with bronchoalveolar lavage improves the diagnostic value of fiberoptic bronchoscopy in this setting.[49]

Specimen Adequacy and Artifacts of Transbronchial Biopsy

In general, bronchoscopists are unable to predict at the time of the biopsy procedure the quality of the specimens obtained based on crude subjective assessments such as whether or not the tissue floats in formalin.[52,53] The use of serrated forceps and the acquisition of multiple (two to four) specimens that fill the forceps cup are the best indicators of a likely diagnostic biopsy.[53,54] For the diagnosis of infection (but not for tumor), a positive correlation was found with the number of biopsy samples obtained and with the presence of at least 20 alveoli in the parenchymal tissue sampled.[55] In a canine study, Shure and associates[56] found no difference in biopsy size, alveolar area, or percentage of alveoli in TBB samples taken at inspiration versus expiration, or in samples consolidated in a tissue cassette prior to placing them in formalin versus samples individually placed immediately in formalin. While the presence of alveolar tissue is necessary to judge a TBB specimen as "satisfactory," there are no good criteria of adequacy when lung parenchyma is present and yet no specific diagnosis can be rendered.[1] Conversely, in a multicompartmental disease such as sarcoidosis, granulomas present in bronchial tissue are

TABLE 1.1. Common artifacts in transbronchial biopsy specimens

1. Lung parenchymal compression
2. Nuclear crush artifact of lymphocytes and tumor cells (especially small cell carcinoma)
3. Sponge artifact
4. Air bubble artifact simulating lipoid pneumonia
5. Acute procedural hemorrhage
6. Telescoping of blood vessels
7. Inadvertent sampling of pleura

diagnostic even when no parenchymal tissue is included in the biopsy sample.[34]

The pathologist should be aware of various histologic artifacts in TBB specimens that may be diagnostically misleading[57] (Table 1.1). Compression of tissue by the biopsy forceps may result in nuclear smearing of inflammatory cell nuclei, mimicking the similarly induced crush artifact of tumor cell nuclei (especially those with small cell carcinoma). Compressed alveolar septa appear hypercellular, simulating interstitial pneumonitis (Fig. 1.2). Kendall and Gal[58] reduced the degree of compression artifact in TBB samples by mechanically stirring the fixative solution during tissue fixation. Sponges in embedding cassettes may produce angulated clefts in the tissue that further impede histological evaluation.[58–61] It is recommended that sponges not be used to secure tissue in cassettes; rather, small tissue fragments should be wrapped in lens paper.[60] Air bubbles of variable size in compressed lung parenchyma create the illusion of exogenous lipoid pneumonia (Fig. 1.2).[1,58] Air-bubble artifact, however, lacks the giant cell reaction and vacuolated histiocytes of lipoid pneumonia (see Chapter 5).[1] Other frequently seen artifacts in TBB specimens are procedure-related acute

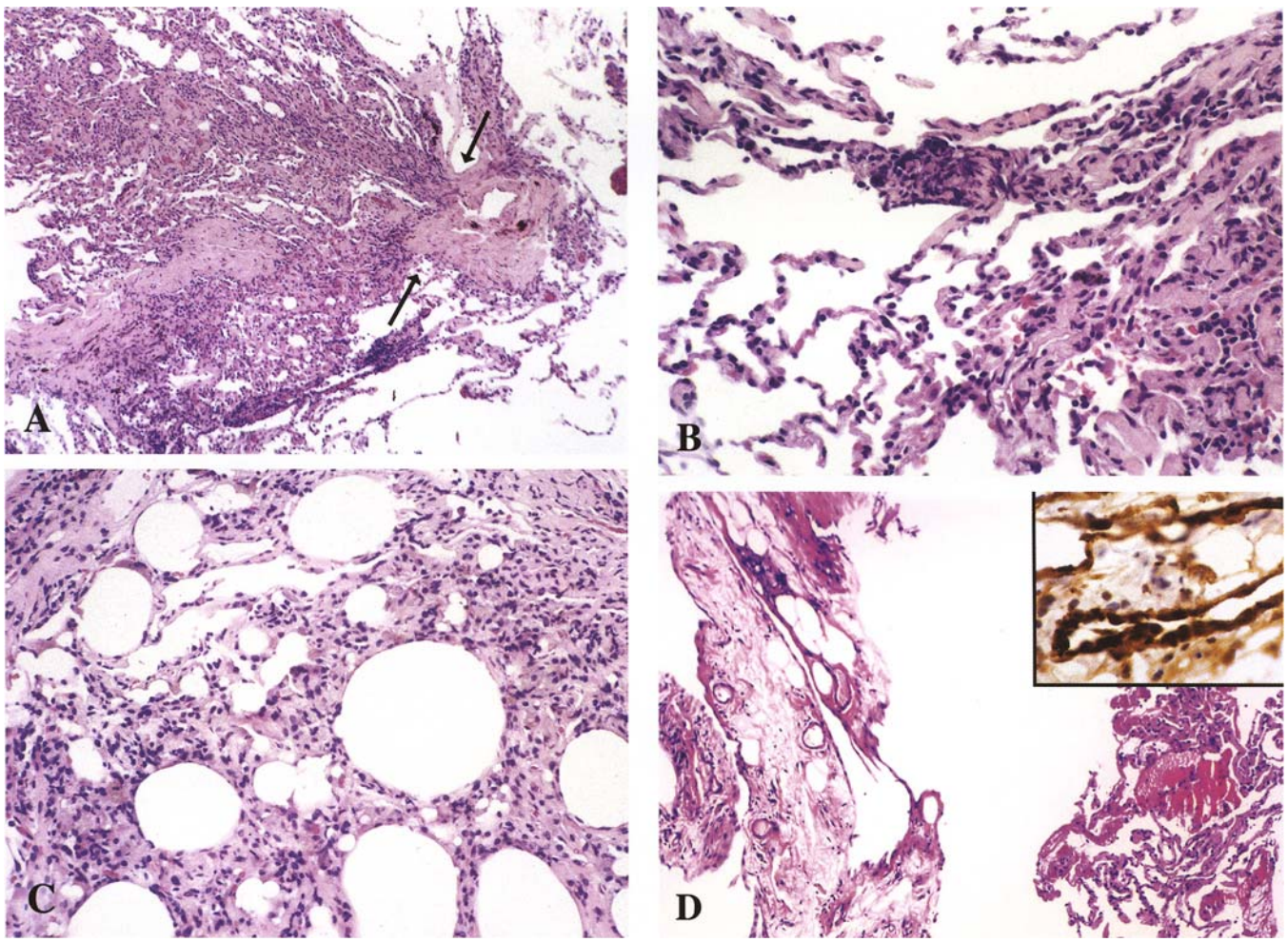

FIGURE 1.2. **A.** Compressed lung parenchyma obtained by transbronchial lung biopsy. The tissue appears pinched from the forceps bite (arrows). **B.** Adjacent areas of expanded and compressed parenchyma in transbronchial biopsy sample. The compressed parenchyma appears hypercellular. **C.** Air bubble artifact simulates exogenous lipoid pneumonia. Air bubbles are surrounded by collapsed lung parenchyma and pigmented macrophages. Note absence of giant cells or other inflammatory reaction. **D.** Fragments of visceral pleura (left) and lung parenchyma (right lower) in this transbronchial biopsy (TBB) sample from patient who developed a post-biopsy pneumothorax. **Inset.** Immunostain for calretinin highlights reactive pleural mesothelial cells.

alveolar hemorrhage, and telescoping of pulmonary vessels that superficially resemble organized thrombi. Infrequently, visceral pleura is inadvertently sampled by TBB, resulting in pneumothorax.[57] Strips of mesothelial-lined connective tissue in a TBB specimen are easily misconstrued as interstitial fibrosis with pneumocyte hyperplasia. An immunostain for calretinin highlights mesothelial cells, while an elastic stain is useful in delineating normal pleural elastic structure in such cases (Fig. 1.2).

Bronchoscopic Transbronchial Needle Biopsy

Bronchoscopic transbronchial needle aspiration (TBNA) was developed by Wang and colleagues[62,63] as a means of obtaining cytologic samples of parabronchial neoplasms or lymph nodes inaccessible to endobronchial forceps biopsy.[64,65] Transbronchial needle aspiration was later applied to sampling intrapulmonary peripheral mass lesions with improved diagnostic yield over TBB alone.[66] A modification of the Wang technique using a larger-caliber needle provides thin tissue cores for histologic assessment.[12,67] In this technique the biopsy needle is positioned endobronchially and pushed through the airway wall into the adjacent lymph nodes or mass lesion.[12,62] For peripheral lesions, a retractable needle is advanced to the lesion under fluoroscopic guidance, a procedure similar to that of TBB.[7,12,66]

The major application of endoscopic TBNA biopsy is in the diagnosis and staging of malignant neoplasms; however, the sampling of juxtabronchial lymph nodes has also been shown to increase the diagnostic yield in stage I sarcoidosis (see Chapter 18).[68,69] Transbronchial needle biopsy specimens tend to be extremely minute and require great care in handling. It is advisable that extra serial sections be prepared at the time of initial histologic sectioning of these minuscule tissue fragments.

Transthoracic Needle Biopsy

Advanced sophisticated radiographic imaging techniques have generated a resurgence in image-guided, percutaneous transthoracic needle biopsies (PTNB), performed by radiologists, of parenchymal nodules, mass lesions, or cysts.[70] Previously, transthoracic needle biopsies using cutting needles or trephines attached to high-speed air drills were done with trepidation because of their high complication rate, including a mortality rate of approximately 0.5% (mainly due to massive hemoptysis or air embolism).[44,71–76] Computed tomography–guided transthoracic needle biopsy is now a much safer procedure with a high diagnostic yield in selected situations.[70,77,78] The addition of automated cutting needles provides cores of tissue that enable a histologic diagnosis and definitive cell typing of malignant neoplasms.[79–81] Tissue cores are processed in the histology laboratory in a similar manner to traditional core biopsy samples of solid viscera such as prostate, liver, or breast. The diagnostic yield of PTNB for malignant lesions ranges from 89% to 93%, with a specificity approaching 100%.[80,81] Percutaneous transthoracic needle biopsy is especially useful in verifying lung metastases in patients with multiple pulmonary nodules and a single known primary.[82] The addition of fine needle aspirate cytology plus histologic evaluation increases the diagnostic yield.[79,83] Specific diagnoses of benign lesions are rendered in about 71% of cases.[81] A major challenge encountered with transthoracic needle biopsies is establishing benignancy when biopsy samples exhibit only nonspecific inflammation and fibrosis. In this situation, complete excision is frequently required in order to exclude a malignant lesion.[84]

Surgical Lung Biopsy

Open Lung Biopsy

The mini-thoracotomy introduced by Klassen et al.[85] in 1949 replaced the full thoracotomy and opened the door for the routine use of diagnostic open lung biopsy in diffuse lung disease. The mini-thoracotomy involves an incision of approximately 8 cm placed in the anterior fourth or fifth intercostal space.[85,86] Subsequent modifications of this procedure include small incisions through the second or third intercostal space (modified Chamberlain procedure), a larger incision through the posterior auscultatory triangle, or even a supraclavicular incision for sampling lesions at the lung apex.[1,87,88] The radiographic distribution of lung disease usually dictates which thoracotomy site is used. Typically at least two areas from different lobes of the lung are sampled. The tissue fragments obtained by this technique measure on the order of 3 to 4 × 2 × 1 cm, are covered by pleura on two sides, and are stapled at the line of excision.[1]

Video-Assisted Thoracoscopic Surgical Lung Biopsy

Around 1910 Jacobaeus first introduced thoracoscopy using a modified cystoscope to lyse pleural adhesions and to biopsy pleural-based tumors.[89,90] The advent of fiberoptic and video technology has led to widespread application of thoracoscopic procedures. Open lung biopsy has now been largely supplanted by VATS lung biopsy, with resultant decreased patient morbidity, reduced length of hospital stay, and less overall cost.[84,90–94] Video-assisted thoracoscopic surgery excisional biopsy of solitary lung nodules has even been advocated as the initial diagnostic procedure for these lesions, thereby providing a rapid definitive diagnosis of malignant and benign disease.[84,95–98] The applications of VATS are expanding to include larger and more complex surgical procedures including lung reduction surgery, lobectomy, and pneumonectomy.[90]

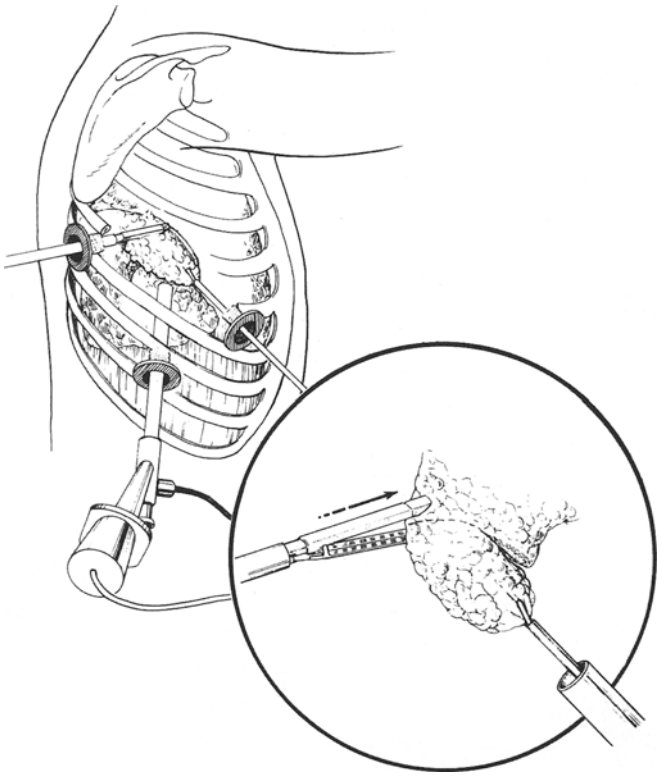

FIGURE 1.3. Thoracoscopic biopsy technique. **Inset.** Videoscopic view of the lung tissue being grasped by the endoscopic forceps introduced through one trocar site and the endoscopic stapler being positioned beneath the grasped tissue as it is introduced through the alternate trocar site. (From Ferson et al.[99] Copyright 1993, with permission from the American Association for Thoracic Surgery.)

Typically, VATS biopsy is performed in the operating room with the patient under general anesthesia and unilateral ventilation of the contralateral lung, resulting in collapse of the manipulated lung.[90] Two to three trocars are introduced into the pleural space to provide access for a thoracoscope with video camera attachment and separate access sites for the thoracoscopic dissecting instruments, grasper, and linear stapler (Fig. 1.3).[90,97,99] The size of the tissue samples obtained and the diagnostic accuracy (92% to 95%) of VATS biopsy are equivalent to that of open lung biopsy (OLB).[91–93,99–101] Histologically, hemorrhage and neutrophil margination are more frequent in VATS biopsy specimens while overinflation is more pronounced in specimens obtained by OLB.[101] These artifacts, however, are minor and do not compromise biopsy interpretation.[101]

Lingular Biopsy

Surgical lung biopsy is considered to be the diagnostic gold standard for diffuse lung disease.[102–104] The diagnostic yield, however, is dependent on adequate sampling by the surgeon. Biopsy of the most diseased area is to be avoided and the selection of areas of average lung involvement, based on direct inspection and knowledge of the radiographic distribution of disease, is advocated.[102] Although the lingula is an attractive site for OLB because of its accessibility, there are concerns that nonspecific inflammation and fibrosis are accentuated in the lingula, rendering it nonrepresentative of the lung as a whole.[103,105] Using a quantitative morphometric grading system of an unselected sample of lungs at autopsy, Newman and colleagues[106] identified increased fibrosis and vascular changes in the lingula compared to other segments. Wetstein,[107] however, found no difference in the diagnostic sensitivity or specificity of lingular biopsies for acute diffuse lung disease. Miller and colleagues[108] likewise found no bias in biopsy samples of the lingula and recommended that the lingula should not be arbitrarily excluded from tissue sampling. They further recommended that a preoperative CT scan should be done routinely to guide the surgeon toward appropriate tissue sampling at the time of OLB.

Handling of Surgical Lung Biopsies

Ideally, surgical lung biopsy specimens should be received fresh from the operating room (OR) to facilitate triaging for diagnostic testing. If tissue for microbiologic cultures has not been submitted directly from the OR, this diagnostic testing should be done at the surgical bench in all nonneoplastic cases. To some extent, the handling of the specimen in the pathology laboratory relates to the clinical situation. If the underlying disease process is thought to represent chronic interstitial lung disease and there is no clinical urgency or a low clinical suspicion of infection, the tissue can be serially sliced and directly placed in fixative for routine histologic processing. Prior inflation of the specimen with fixative introduced transpleurally through a narrow-gauge needle has been advocated as a means of overcoming collapse artifact.[109]

Surgical biopsy samples from patients for whom an immediate diagnosis is clinically necessary, such as patients with acute lung injury, immunosuppression, or suspected infection, as well as from patients with possible lymphoma, vasculitis, or lung hemorrhage, should be initially evaluated with cytologic touch imprints and diagnostic frozen section according to the flow diagram presented in Figure 1.4. While awaiting the frozen section, the touch imprint of the freshly sliced specimen can be fixed immediately in absolute alcohol and then stained rapidly with H&E for assessment of malignant cells, inflammatory cells, or pathogens. A rapid Gomori methenamine silver (GMS) stain of the touch imprint, available within an hour, may be screened for *Pneumocystis* and other fungal organisms.[110] The histologic pattern of lung disease is assessed on the frozen section slide, and the

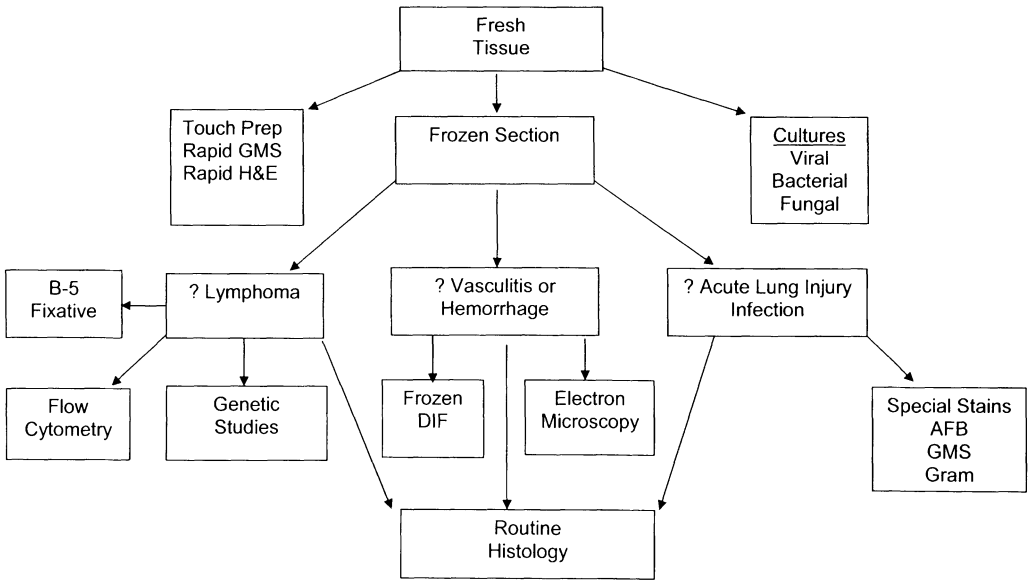

FIGURE 1.4. Flow chart for the handling of urgent or emergent surgical lung biopsy specimens in cases of acute lung injury, infection, alveolar hemorrhage/vasculitis, or lymphoma (see text). AFB, acid-fast bacillus; DIF, direct immunofluorescence; GMS, Gomori methenamine silver (stain); H&E, hematoxylin and eosin.

specimen can then be properly allocated for necessary ancillary testing (Fig. 1.4). The handling of lung biopsy specimens in cases of suspected lymphoma is further described in Chapter 32. In cases where infection is suspected, stains for microorganisms should be ordered at the time of accessioning and reviewed on the permanent sections as early as possible the following day.

Diagnostic Yield of Surgical Lung Biopsies

The diagnostic yield of surgical lung biopsies relates to the underlying immune status of the patient, that is, whether the patient is immunosuppressed or immunocompetent. Patients may be immunosuppressed for a wide variety of reasons, including an underlying malignancy or its treatment with chemotherapy or radiotherapy; steroid or other immunosuppressive therapy for nonneoplastic conditions, such as autoimmune diseases and other inflammatory states; organ transplantation; or congenital immunodeficiency disorders.[111] Patients with AIDS are subject to a different pathologic spectrum of diseases than are non-AIDS immunosuppressed patients. Because of the greater severity of immunodepression in patients with AIDS, the causes of lung infection, the tissue reaction patterns to the causative organism(s), and the greater tissue burden of microorganisms defines the AIDS population.[1,112]

Immunosuppressed patients frequently develop localized or diffuse lung infiltrates that are initially evaluated by traditional diagnostic procedures such as sputum cultures, bronchial washings and brushings, and TBB. Surgical lung biopsy is performed after these less invasive procedures fail to yield a diagnosis, or when the patient's clinical course rapidly deteriorates. In a previous review of 18 major series of TBB or OLB in non-AIDS immunosuppressed patients, Dail[1] found that the major diagnostic categories were infection and malignant neoplasms.[113–130] Infection was diagnosed in 10% to 96% (median, 42%) of biopsies, respectively. The percentage of nonspecific diagnoses among the 19 series ranged from 0% to 66% (median, 40%) of biopsies, and the mortality rate was high (15% to 74% of patients, respectively).[1,113–130]

The clinical benefit of a specific diagnosis on OLB in the immunosuppressed population has been questioned.[120,131] Rossiter and colleagues[120] found that of those patients for whom lung biopsy dictated a change in treatment, 22% died in the hospital compared to 28% of patients in whom no treatment change was indicated after OLB. These authors also found that patients whose biopsies yielded a specific diagnosis fared no better than those without a specific diagnosis (26% vs. 24% mortality). Surgical lung biopsy is now a mainstay in the evaluation of immunosuppressed patients, and the opportunity to establish the efficacy of this procedure in prospective clinical trials has realistically been lost.[131] It is therefore important that each patient be critically evaluated prior to undertaking a surgical lung biopsy to assess the likelihood that the biopsy will be diagnostic, and if diagnostic, whether or not the patient's outcome will be improved.[131–133] Surgical lung biopsy should also be undertaken as early as possible in the patient's clinical course.

Nonimmunocompromised patients with chronic or subacute diffuse infiltrative lung disease, the so-called non–critically ill group, may also require a diagnostic surgical lung biopsy.[41] In the large progressive series of patients studied by Gaensler and colleagues,[38,102,103] approximately one third of patients with diffuse infiltrative diseases required lung biopsy for diagnosis. In the series of Ray et al.,[105] which included 416 OLBs, patients exhibited the symptoms of cough (71%), dyspnea (61%), chest pain (40%), and weight loss (40%). This category of patients typically has chest radiographs that show either a mass effect, persistent localized infiltrate or diffuse interstitial disease. Of the 502 patients, reported by Gaensler and colleagues[103] who underwent OLB for chronic diffuse infiltrative lung disease, nonspecific changes were identified in 5.6%, normal lung in 0.8%, and exclusively honeycomb lung in 3.4% of OLB samples, for an overall diagnostic yield of 90%. Other series have also shown the diagnostic yield of surgical lung biopsy in the nonimmunosuppressed population to range from 95% to 100%.[101,134,135] Occasionally surgical lung biopsy is necessary for patients with symptoms and pulmonary function abnormalities but with normal chest radiographs.[136] In this group, changes of desquamative interstitial pneumonia or extrinsic allergic alveolitis were most often found.[103,136]

Temes and colleagues[137] studied the efficacy of surgical lung biopsy related to clinical urgency in a series of patients, most of whom were immunocompetent. For stable patients undergoing elective procedures and in those for whom the biopsy was considered to be urgent, beneficial therapeutic changes were made on the basis of surgical lung biopsy and operative mortality was low. In patients undergoing an emergency biopsy, mortality rate was high (54%) and therapeutic changes consisted of the addition of steroids in 82%. On the basis of this study, emergency surgical lung biopsy in this group of patients was considered to be disadvantageous.[137] The efficacy and diagnostic yield of surgical lung biopsy in patients with acute respiratory distress syndrome is covered in Chapter 4.

The Normal or Minimally Abnormal Surgical Lung Biopsy

Occasionally the slides of a surgical lung biopsy specimen demonstrate apparently minimal histologic changes in the face of significant clinical or radiographic findings (Table 1.2). This situation may be the result of inadequate tissue sampling. Certain clinical conditions, however, have been notably associated with minimal changes on surgical lung biopsy.[138] Early interstitial edema due to congestive heart failure or noncardiogenic edema may present histologically with subtle expansion of interlobular septa and dilated lymphatics.[138] Among the chronic diffuse infiltrative disorders, pulmonary Langerhans' cell granulomatosis occasionally presents with minimal changes in surgical lung biopsy specimens because of aberrant sampling of widely dispersed cellular lesions.[138] Prior treatment of interstitial pneumonia with steroids may also suppress inflammatory changes, leaving only slight lymphocytic perivascular cuffing and type II pneumocyte hyperplasia in the biopsy slide.[138] Pulmonary hypertension sometimes presents with restrictive changes on lung function tests, yet histologically vascular sclerosis may be the only abnormality seen.[139] Biopsy samples of rounded atelectasis may be submitted as a suspected neoplasm or mass lesion, but histologically only collapsed lung parenchyma and thickened pleura are observed (see Chapter 27). Restriction due to extrapulmonary causes such as obesity or neuromuscular disease will have minimal associated histologic changes in the lung. Close correlation of the histologic findings with clinical and imaging data; scrutiny of the slides for subtle features of interstitial edema, chronic congestive heart failure, bronchiolitis, or pulmonary hypertensive vascular disease; and deeper sections or rotation of the block to disclose widely dispersed lesions may resolve the frustrating dilemma of a "minimal change" OLB.

TABLE 1.2. Causes of minimally abnormal surgical lung biopsy specimen*

1. Surgical sampling error of dispersed lesions (especially Langerhans' cell (histiocytosis)
2. Pulmonary edema
3. Pulmonary hypertension
4. Bronchiolar disease
5. Prior immunosuppressive therapy
6. Fat emboli
7. Rounded atelectasis
8. Extrapulmonary restriction

*See Colby and Yousem.[138]

Resection Specimens

Surgical lung resection, including segmental, lobar, or whole lung removal, is usually performed for the excision of a malignant neoplasm, but occasionally is required for advanced nonneoplastic disease, including lung transplant. The best method for processing large lung specimens of all types is to fix the lung in inflation followed by serial slicing. Inflation-fixation provides for excellent histologic detail of lung parenchyma, most clearly defines the location of lesions and their anatomic relationships, and enables superior radiographic-pathologic correlation. Inflation-fixation is indispensable for the evaluation of pulmonary emphysema. In a busy surgical pathology laboratory, inflation-fixation for as little as 1 hour ade-

quately preserves anatomic detail, but overnight fixation, if possible, is recommended. The need for fresh lung tissue for special studies or microbiologic cultures must be anticipated and the tissue obtained prior to fixation. The acquisition of fresh lung samples does not usually preclude inflation-fixation since small pleural tears or punctures do not severely hamper lung inflation, and larger pleural defects can be sutured or closed with small clamps.[140]

In resections for neoplasm, the bronchial margin should be sectioned and the peribronchial lymph nodes sampled prior to inflation-fixation. The lung is then weighed, placed in a large container, and distended through the bronchus with 10% neutral buffered formalin (or other preferred fixative) introduced via a tube attached to an elevated reservoir of fixative until the pleural surface is fully expanded and smooth. The distance between the lung and the reservoir should be about 25 cm. It is convenient to have available an assortment of cannulae of different sizes to provide a tight bronchial seal. Removal of intrabronchial mucus or manipulation of the tubing within the bronchus is sometimes required to effect inflation of all bronchopulmonary segments. For severely atelectatic lungs, gentle kneading of the lung parenchyma during fixation, or leaving the specimen attached to the fixative reservoir for a prolonged interval is helpful. Once the lung is fully expanded the cannula can be removed and the bronchus either clamped or sealed with a cotton plug and the lung covered with fixative in a nonrestrictive, closed container. Suspension of the lung from the lid of the container eliminates the possibility of compression artifact.

After fixation the pleural surface should be completely inspected and the external anatomic landmarks documented. If parietal pleura or chest wall is attached to the specimen, the surgical margins of these structures are sampled. Samples should also be obtained from all pleural stapled margins. This can be readily accomplished by trimming the tissue on the surface of the staples with fine pediatric dissecting scissors. The lung is then serially sliced at 1-cm intervals (or 0.5-cm intervals for pediatric lungs) using a long sharp slicing knife. A simple cutting board with elevated 1-cm edges is ideal for obtaining uniformly thick slices (Fig. 1.5). The lung should be cut in the plane most suitable to display the neoplasm and its extension, or for optimal radiographic correlations. Initially bisecting the lung in the appropriate plane facilitates subsequent slicing. In our laboratory we routinely slice lungs in the coronal plane to correlate with the posteroanterior chest radiograph. Correlations with CT scans are best achieved by cutting the lung in the horizontal plane.

Lung slices are next oriented and arranged sequentially on a large tray, inspected, and sampled for histologic review. Photographs may be taken prior to histologic sectioning or, alternatively, one of two adjacent mirror-image slices can be sampled and the other preserved for photography. In evaluating lung neoplasms, the specimen should be assessed for pathologic staging (see Chapter 35). The tumor should be precisely localized according to the bronchopulmonary segments, measured, and sampled (at least one section per centimeter) for histology. The relationships and distances between the tumor and the overlying pleura, interlobar fissures, and nearest bronchi should be recorded and documented histologically. Any additional lymph nodes should be sampled and their anatomic position noted. It is important to next assess the parenchyma, documenting the presence of satellite lesions and the gross extent of emphysema, fibrosis, pneumonia, or any other macroscopic abnormalities. Histologic sampling of the parenchyma should include representative sections from each lobe, including each grossly distinctive type of anatomic lesion in addition to at least one sample of the most normal-appearing parenchyma. Using this approach, the often neglected, nonneoplastic "second diagnosis" will be included in the surgical pathology report.[141] An example of histologic sampling in a case of resected lung cancer is presented in Figure 1.6.

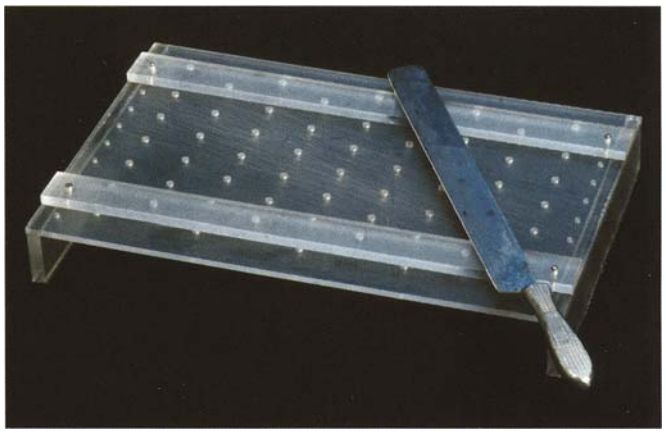

FIGURE 1.5. Plexiglas lung cutting board. Note holes for fluid drainage and movable 1-cm-thick runners for obtaining uniformly thick lung slices.

Resection specimens for nonneoplastic disease are processed in a similar manner as neoplastic specimens, but usually without the need for sampling the specimen margins. In cases of suspected infection, appropriate microbiologic cultures must be obtained prior to fixation. The parenchymal sampling protocol in nonneoplastic cases should be directed toward the major underlying disease process. At least one cross section of central airway should be obtained for histologic assessment of airway pathology and mucous gland hyperplasia. The sampling protocol for pneumoconioses, including acquisition of tissue for mineralogic analysis, is presented in the review by Gibbs and Seal.[142]

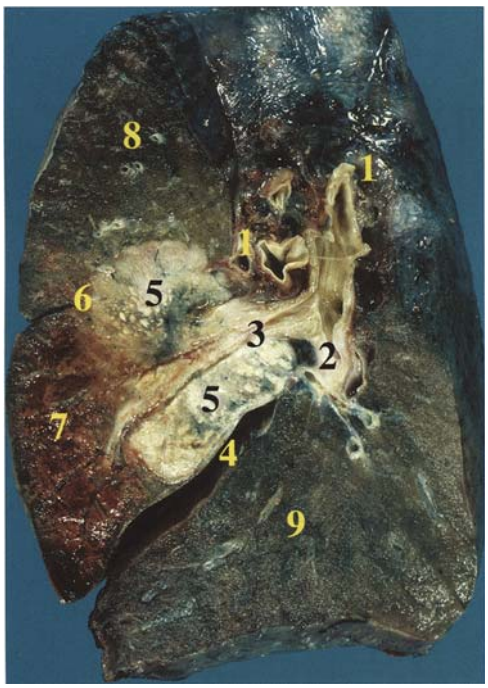

FIGURE 1.6. Example of histologic sampling of a right pneumonectomy specimen for non–small-cell carcinoma. 1, bronchial and vascular margins; 2, lymph nodes; 3, endobronchial tumor extension; 4, pleural edge nearest the tumor; 5, representative sections of tumor; 6, tumor extension across minor fissure; 7, obstructive pneumonia; 8 and 9, representative sections of parenchyma of upper and lower lobes (see text).

Autopsy Specimens

The handling of intact whole lungs removed at autopsy is identical to that described for large surgical resections, that is, inflation-fixation followed by serial slicing. A common autopsy practice is to examine and dissect one lung in the fresh state and the other after inflation-fixation. The nonexpanded lung is felt to better represent pneumonia and pulmonary edema. In reality, as long as the lung is weighed and cultured prior to fixation, in my experience, inflation-fixation of bilateral lungs is optimal. If only one lung is to be fixed in inflation, the most diseased lung should be selected.

Dissection of the noninflated lung can be accomplished by initially opening the bronchi from hilus to periphery followed by slicing the lung sagittally. Sagittal slicing provides many cross sections of bronchi and vessels, allowing for optimal study of these structures.[143] The lung may alternatively be sliced in the coronal plane, leaving the slices attached at the hilum and parahilar area, thus preserving anatomic relationships. A third alternative approach is dissection of bronchi and vessels from incisions made along the lateral surfaces of the lung.[143] While this method is technically more difficult, it leaves the dissected lung in continuity, allowing for reconstruction of lesions.[143]

Since the focus of the autopsy is directed toward a determination of the cause of death, as well as an assessment of the effects of medical or surgical therapy or possible iatrogenic lung injury, and the provision of detailed clinical-pathologic correlations, there are unique considerations related to the handling and removal of the lung postmortem that do not apply to the surgically excised lung.[144] A careful review of the available medical records and radiologic reports prior to starting the autopsy is important so that the prosector can anticipate suspected pulmonary diseases and appropriately test for them. The evaluations for pneumothorax, gas embolism, upper airway obstruction, and suspected anaphylaxis require special procedures that must be performed prior to lung removal (see Chapter 31). In-situ dissection of the pulmonary trunk and main pulmonary arteries should be carried out in cases of suspected pulmonary embolism, and the leg veins dissected if emboli are found. In cases of suspected bronchoesophageal fistula, the esophagus should remain attached to the posterior aspect of the thoracic block during its removal.

Intrathoracic fluid must also be carefully measured, described, and appropriately cultured. A hematocrit should be obtained when the fluid is hemorrhagic. All intrathoracic catheters and cannulae, including chest tubes, endotracheal tubes, and pulmonary artery catheters, should be localized and their positions documented. Iatrogenic lung laceration or perforation by chest tubes occasionally escapes clinical recognition (see Fig. 7.5 in Chapter 7).[145] Localized lung parenchymal hemorrhage due to pulmonary arterial perforation by a pulmonary artery catheter has a distinctive macroscopic and histologic appearance.[146] The deleterious effects of endotracheal intubation and mechanical ventilation should also be assessed at autopsy.

A special situation related to removal of the lung postmortem is the presence of dense pleural adhesions, fibrothorax, or a pleural-based neoplasm that tightly adheres the lung to the chest wall. In this setting, extrapleural dissection, in which the lung is removed with its complete pleural investment, is accomplished by sharp dissection between the thickened parietal pleura and the rib cage. Attempts to separate the lung from the parietal pleura by blunt or sharp dissection invariably result in lacerations, which induce artifact and prevent adequate inflation-fixation.

In cases of suspected pneumoconiosis, a semiquantitative macroscopic assessment, including type, size, and profusion of lesions, should be recorded for dust foci, emphysema, and interstitial fibrosis (see Chapter 26).[142] The recommended sampling protocol for asbestos-related lung disease is that of the pneumoconiosis panel of the College of American Pathologists (see Chapter 27).[147]

Special Techniques

Numerous techniques have been applied to lungs mainly obtained at autopsy in order to study in detail varied aspects of pulmonary pathology. This section describes some of the more practical and useful techniques, and provides references for the interested reader. Those methods that I consider particularly applicable or have personally utilized are discussed in more detail. A good general review of supplemental methods for examining lungs can be found in Ludwig's[143] *Handbook of Autopsy Practice*, and in the article by Whimster.[148] Space limitations prohibit a detailed discussion of morphometric techniques and the processing of lungs for quantitative evaluation. The classical principles and application of lung morphometry can be found in the authoritative text by Weibel.[149] A practical approach to the quantitative study of lung pathology has been provided by the British Medical Research Council Committee headed by Dunnill et al.[150]

Rapid Giant Paper Sections of Lung

In 1949 Gough and Wentworth[151] described a method for preparing whole lung sections mounted on paper. This technique has been applied extensively to the study of emphysema and pneumoconioses. A modification of this method by Whimster[152] reduces the time required for preparation, making the technique more readily available for general laboratory use. The rapid method requires formalin inflation-fixation followed by serial slicing of the lung as previously described. One or more thick lung slices is then embedded in gelatin, frozen, and cut thinly (400 to 600 µm) with a rotary meat slicer. The thin slice is then rinsed, mounted with gelatin on paper, and dried. The section may be stained or remain unstained, and is available for viewing after 24 to 48 hours.[152] Air-space dilatation and the pigmented macular and fibronodular lesions of pneumoconioses are readily discerned and quantified (see Fig. 26.8 in Chapter 26). The paper-mounted section can be included as a permanent record with the autopsy report.

Barium-Sulfate Impregnation

This simple technique advocated by Heard[153,154] enhances the gross detection of emphysema and other parenchymal lesions in slices of inflated fixed lung. Representative lung slices are alternately immersed for approximately 30 seconds each in warm saturated aqueous solutions of barium nitrate (75 g/L) and sodium sulfate (100 g/L). The lung is gently squeezed to promote uptake of each solution, and as much fluid as possible is manually expressed immediately before immersion in the alternate solution.

FIGURE 1.7. Lung parenchyma showing severe mixed panacinar emphysema and fibrosis. Relatively normal lung parenchyma is seen in the left upper corner. Barium-sulfate impregnation. Photograph taken of lung immersed in water.

After about three immersion cycles a homogeneous white-gray precipitate coats the surface of the lung slice and enhances the normally translucent surface features. Following barium-sulfate impregnation the lung is then submerged in water in a glass dish and can be examined to great advantage with a hand lens or dissecting microscope. Exquisite macroscopic photographs can be taken of the submerged lung (Fig. 1.7). Histologic structure is preserved, although barium-sulfate particles can be seen along tissue surfaces.

Injection Cast Methods

Barium-Sulfate-Gelatin Vascular Injection

The distribution, branching pattern, and macroscopic structure of the pulmonary vasculature are well studied by vascular injection methods. Barium-sulfate-gelatin injection has been used extensively by Reid and colleagues[155,156] to study the pulmonary vasculature during lung development and in various disease states of children and adults. In this method the pulmonary arteries (or veins) of the fresh lung are injected for 4 to 7 minutes with a suspension of barium sulfate and gelatin heated to 60°C and applied at a pressure of approximately 100 cm H_2O. It is important that the lung be brought to room temperature and overlaid with a heating pad to ensure free flow of the injection mixture. This casting method fills vessels down to about 15 µm in diameter without entering the capillary bed. Following injection the lung is then fixed in inflation, and specimen radiography is performed on the intact lung and sequential lung slices to display vascular branching patterns (Fig. 1.8). Lungs prepared in

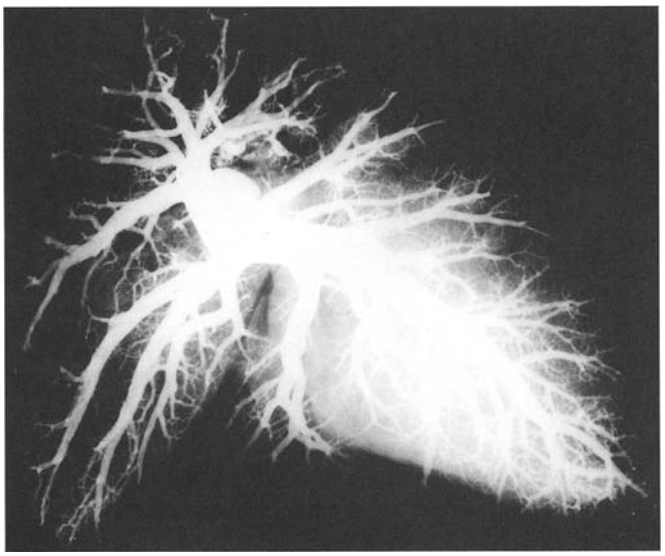

FIGURE 1.8. Postmortem whole lung arteriogram from patient with cystic fibrosis and cor pulmonale. Note the widened central arteries and the peripheral pruned branches with a striking reduction in background haze in the upper lobe (left). Barium-sulfate-gelatin vascular injection. (From Tomashefski JF Jr, et al. Pulmonary pathology. In: Hodson ME, Batten JC, eds. Cystic fibrosis. London: Bailliere Tindall, 1983:40, with permission.)

this way are ideal for subsequent histologic study and vascular measurements since the vessels are marked and fully distended by the gelatin mixture.

Corrosion-Casting Techniques

The basic concept of corrosion casting is the filling of a hollow space by a fluid material that hardens, followed by digestion of the surrounding tissue. This modality facilitates detailed study of anatomic organization in three dimensions, and has been used to study the pulmonary vasculature, lymphatics, and airways (Fig. 1.9).[1,157,158] Casting materials include wax, metals, gelatin, celloidin, neoprene, vinylite, latex, silicone, and acrylic products.[1,159–161] Different anatomic compartments within the same organ can be studied simultaneously by the injection of material containing contrasting colors, illustrating different anatomic structures to maximal efficiency. The negative aspect of corrosion-casting techniques is destruction of lung parenchyma, which precludes histologic examination.

Vinylite casts were used extensively in the laboratory of Averill Liebow in studies of the pulmonary vasculature, collateral blood supply, bronchial arterial system, and bronchiectasis (Fig. 1.9). The interested reader is

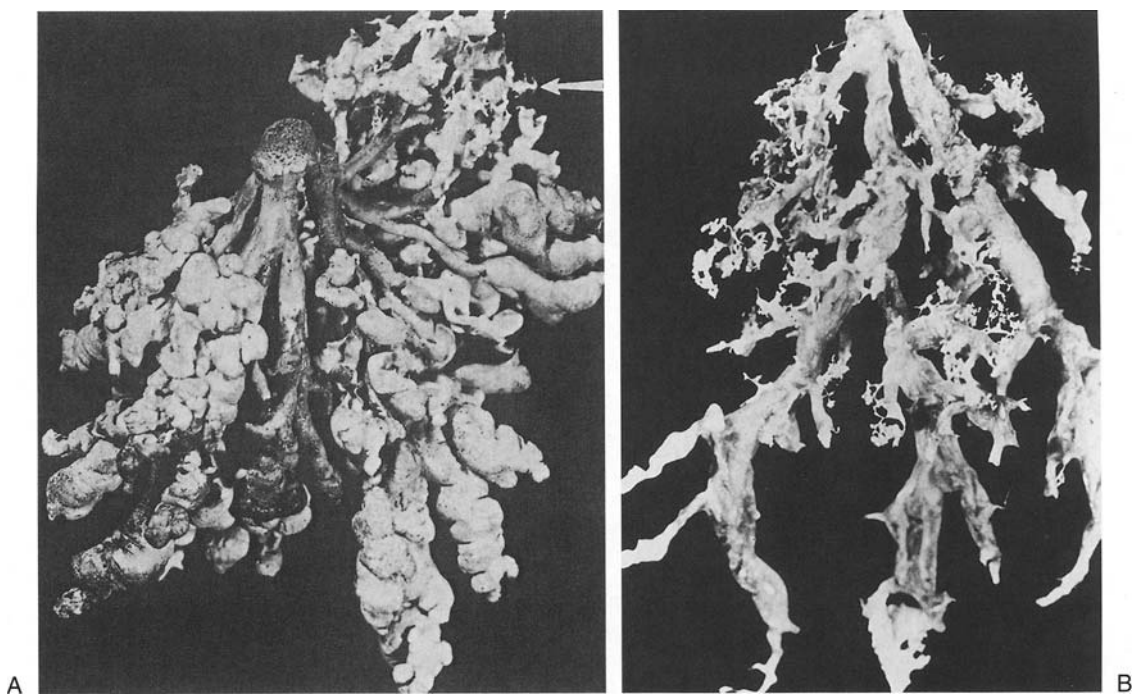

FIGURE 1.9. Corrosion cast of bronchial tree in nonobstructive bronchiectasis. **A.** Saccular bronchiectasis. Less severe damage is present in upper part. (From Liebow et al.,[158] with permission.) **B.** Varicose bronchiectasis. Note irregular involvement and irregular contours of dilated bronchi. Also note persistence of connections to lung as evidenced by smaller areas of injection material. (Courtesy of A.A. Liebow Pulmonary Pathology Collection, San Diego, CA.)

referred to the review by Dail[1] and to the article by Liebow and colleagues[158] in which this technique is described.

Specimen Inflation-Fixation Methods

Formalin Inflation Tank

For anatomic laboratories with a high volume of lung specimens, and for protocols that necessitate precise specimen inflation such as required for morphometric studies, a specimen inflation tank may be considered. As described by Heard et al.,[153,162] the basic construct includes a large inflation tank filled with formalin, and a smaller formalin supply reservoir elevated a distance above the tank to ensure a delivery pressure head of about 25 cm. The reservoir is connected by plastic tubing to a manifold to which can be attached multiple lung specimens simultaneously. An electrical pump automatically recycles fixative from the inflation tank to the reservoir, in which the level of fixative is regulated by a float sensor, to maintain the pressure column throughout fixation (Fig. 1.10). Because of the large volumes of formaldehyde that are used, the apparatus must be located under a fume hood. Due to evaporation, the tank must also be refilled periodically and the concentration of formaldehyde within the tank monitored.

Formalin Fume Fixation

Formalin fume fixation as a means of inflation-fixation with maximal preservation of lung volumes and anatomic relationship was proposed by Blumenthal and Boren[163] in 1959. By means of an air source bubbled through formaldehyde at 5 to 30 L/min, vaporized formalin can be passed through the distended lung for 3 to 5 days. Using this method the final product is an expanded lung that is rigid and dry, having the consistency of Styrofoam. The lung may be sliced with a knife or a band saw. Acceptable histologic sections can be obtained, and the method is excellent for producing thick sections that can be studied in three dimensions.[163]

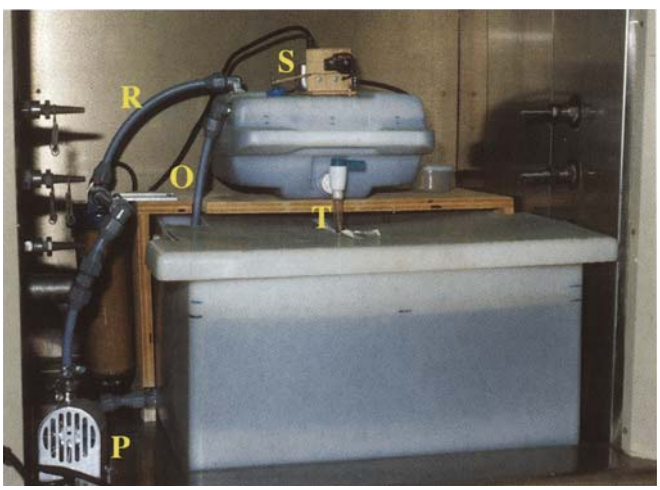

FIGURE 1.10. Formalin inflation tank. Large plastic tank filled with formalin, with overriding smaller plastic formalin reservoir. P, circulating pump; R, recirculation tube; S, float sensor; O, overflow channel; T, tubing connected to multiport manifold (not visualized) located in the bottom of the tank.

FIGURE 1.11. Severe bullous panacinar emphysema. Section of dried lung after formalin fume fixation. (Prepared in the laboratory of Dr. Philip Pratt.)

Variations on the method of formalin fume fixation have been described by Markarian,[164] Pratt,[165] Wright and colleagues,[166] and Weibel and Vidone.[167] The Pratt modification allows the postmortem lung to "breathe" formalin vapors by means of a ported cylinder and piston. Pratt and Klugh[168] utilized this inflation apparatus to perform postmortem lung function tests that were correlated with the pathologic anatomy of the fixed lung (Fig. 1.11). Fume fixation techniques are primarily research methods that require construction of rather elaborate inflation devices, and necessitate venting of toxic formaldehyde fumes.

Tracheobronchial Whole Mounts

To study the structure and distribution of cartilage plates in the tracheobronchial tree, whole mounts of the airway can be selectively stained for cartilage and then cleared. According to the method of Landing and Wells,[169,170] the

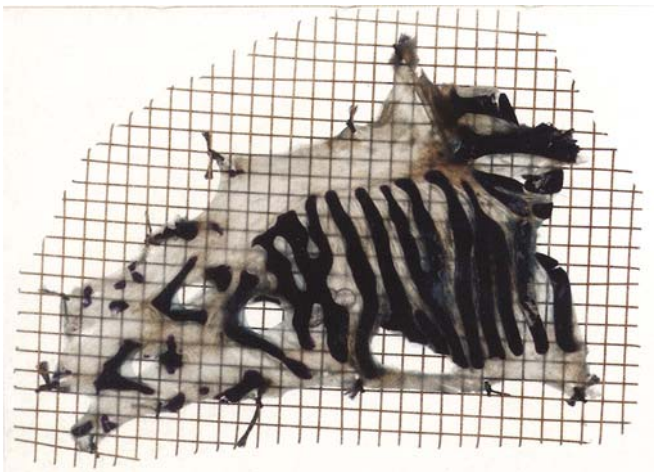

FIGURE 1.12. Whole mount of opened, normal adult right lower lobe bronchus and bronchus intermedius stained with toluidine blue to highlight cartilage plates. (Specimen prepared by Dr. Bal Kampalath.)

dissected airway is immersed in a dilute toluidine blue solution, followed by clearing of the tissue in graded ethanol (70% to 95%) and finally xylene. Toluidine blue impregnates the cartilage with a deep blue color. Loosely adherent stain is removed from the connective tissue by the solvent rinses during the clearing process, allowing the cartilage to stand out in the translucent airway wall (Fig. 1.12). The specimen can then be secured to wire mesh and preserved in mounting medium or clear plastic.

The technique of tracheobronchial whole mounts was used by Landing and colleagues[169] and others[170,171] to study tracheobronchial anomalies, including those seen in congenital lobar emphysema (see Chapter 6). Tracheobronchial whole mounts of adult airways have also been studied to document atrophy of cartilage in chronic obstructive lung disease.[172,173] In my experience, staining for cartilage is inconsistent in adult bronchi that have been fixed in formalin for prolonged periods.

Assessment of Cardiac Ventricular Weights

Although not a technique applied to the lung, the measurement of cardiac ventricular weights is often an important adjunct to assess right ventricular hypertrophy in conditions of suspected pulmonary hypertension and cor pulmonale. Simple linear measurement of the thickness of the right ventricular free wall is notoriously inaccurate for establishing right ventricular hypertrophy. The preferred method for determining ventricular weights is that of Fulton, Hutchinson, and Jones,[174] in which the right ventricular (RV) free wall and left ventricle plus septum (LV+S) are dissected free of the heart and from each other and weighed separately after removal of epicardial fat and coronary arteries. Individual ventricular weights and the ratio of RV to LV+S are determined. In general, for isolated right ventricular hypertrophy, an absolute RV weight exceeding 80 g or an RV/LV+S ratio >0.5 establishes the diagnosis.[174] A deficiency of this method is that the RV/LV+S ratio is invalid as a measure of right ventricular hypertrophy when there is also left ventricular hypertrophy. The method of Fulton et al.[174] has also been applied to the study of the heart during fetal development.[175]

References

1. Dail DH. Tissue sampling. In: Dail DH, Hammar SP, eds. Pulmonary pathology. 2nd ed. New York: Springer-Verlag, 1993:1–19.
2. Andersen H. Transbronchial lung biopsy for diffuse pulmonary diseases. Results in 939 patients. Chest 1978;73: 734–736.
3. Haponik EF, Summer WR, Terry PB, Wang KP. Clinical decision making with transbronchial lung biopsies. The value of nonspecific histologic examination. Am Rev Respir Dis 1982;125:524–529.
4. Taylor CR, Shi S-R, Barr NJ, Wu N. Techniques of immunohistochemistry: principles, pitfalls and standardization. In: Dabbs DJ, ed. Diagnostic immunohistochemistry. Philadelphia: Churchill Livingstone, 2002:3–43.
5. Prakash VBS, Stubbs SE. The bronchoscopy survey: some reflections. Chest 1991;100:1660–1667.
6. Prakash VBS, Offord KP, Stubbs SE. Bronchoscopy in North America: The ACCP Survey. Chest 1991;100:1668–1675.
7. Boyd AD. Endoscopy: bronchoscopy and esophagoscopy. In: Sabiston DC Jr, Spencer FC, eds. Surgery of the chest. 6th ed. Philadelphia: WB Saunders, 1995:69–97.
8. Ikeda S. Flexible bronchofiberscope. Ann Otol Rhinol Laryngol 1970;79:916–923.
9. Thompson AB, Rennard SI. Diagnostic procedures not involving the pleura. In: Baum GL, Crapo JD, Celli BR, Karlinsky JB, eds. Textbook of pulmonary diseases. 6th ed. Philadelphia: Lippincott-Raven, 1998:239–253.
10. Zavala DC. Transbronchial biopsy in diffuse lung disease. Chest 1978;73(suppl):727–733.
11. Kovnat DM, Rath GS, Anderson WM, Snider GL. Maximal extent of visualization of bronchial tree by flexible fiberoptic bronchoscopy. Am Rev Respir Dis 1974;110: 88–90.
12. Shure D. Transbronchial biopsy and needle aspiration. Chest 1989;95:1130–1138.
13. Shure D, Astarita RW. Bronchogenic carcinoma presenting as an endobronchial mass. Optimal number of biopsy specimens for diagnosis. Chest 1983;83:865–867.
14. Zavala DC. Diagnostic fiberoptic bronchoscopy: techniques and results of biopsy in 600 patients. Chest 1975; 68:12–19.

15. Popovich J Jr, Kvale PA, Eichenhorn MS, Radke JR, Ohorodnik JM, Fine G. Diagnostic accuracy of multiple biopsies from flexible fiberoptic bronchoscopy. A comparison of central versus peripheral carcinoma. Am Rev Respir Dis 1982;125:521–523.
16. Zavala DC. Pulmonary hemorrhage in fiberoptic transbronchial biopsy. Chest 1976;70:584–588.
17. Herf SM, Suratt PM, Arora NS. Deaths and complications associated with transbronchial lung biopsy. Am Rev Respir Dis 1977;115:708–711.
18. Radke JR, Conway WA, Eyler WR, Kvale PA. Diagnostic accuracy in peripheral lung lesions. Factors predicting success with flexible fiberoptic bronchoscopy. Chest 1979; 76:176–179.
19. Ellis JH Jr. Transbronchial lung biopsy via the fiberoptic bronchoscope. Experience with 107 consecutive cases and comparison with bronchial brushing. Chest 1975;68: 524–532.
20. Lai RS, Lee SS, Ting YM, Wang HC, Lin CC, Lu JY. Diagnostic value of transbronchial lung biopsy under fluoroscopic guidance in solitary pulmonary nodule in an endemic area of tuberculosis. Respir Med 1996;90:139–143.
21. Milman N, Farschou P, Munch EP, Grode G. Transbronchial lung biopsy through the fibre optic bronchoscope. Results and complications in 452 examinations. Respir Med 1994;88:749–753.
22. Hanson RR, Zavala DC, Rhodes ML, Keim LW. Transbronchial biopsy via flexible fiberoptic bronchoscope: results in 164 patients. Am Rev Respir Dis 1976;114: 67–72.
23. Popp W, Rauscher H, Ritschka L, Redtenbacher S, Zwick H, Dutz W. Diagnostic sensitivity of different techniques in the diagnosis of lung tumors with the flexible fiberoptic bronchoscope. Comparison of brush biopsy, imprint cytology of forceps biopsy, and histology of forceps biopsy. Cancer 1991;67:72–75.
24. Andersen HA, Fontana RS, Harrison EG Jr. Transbronchoscopic lung biopsy in diffuse pulmonary disease. Dis Chest 1965;48:187–192.
25. Koerner SK, Sakowitz AJ, Appelman RI, Becker NH, Schoenbaum SW. Transbronchial lung biopsy for the diagnosis of sarcoidosis. N Engl J Med 1975;293:268–270.
26. Koontz CH, Joyner LR, Nelson RA. Transbronchial lung biopsy via the fiberoptic bronchoscope in sarcoidosis. Ann Intern Med 1976;85:64–66.
27. Poe RH, Israel RH, Utell MJ, Hall WJ. Probability of a positive transbronchial lung biopsy result in sarcoidosis. Arch Intern Med 1979;139:761–763.
28. Halme M. Piilone A, Taskinen E. Comparison of endobronchial and transbronchial biopsies with high-resolution CT (HRCT) in the diagnosis of sarcoidosis. APMIS 2001; 109:289–94.
29. Aranda C, Sidhu G, Sasso LA, Adams FV. Transbronchial lung biopsy in the diagnosis of lymphangitic carcinomatosis. Cancer 1978;42:1995–1998.
30. Housini I, Tomashefski JF Jr, Cohen A, Crass J, Kleinerman J. Transbronchial biopsy in patients with pulmonary eosinophilic granuloma. Comparison with findings on open lung biopsy. Arch Pathol Lab Med 1994;118: 523–530.
31. Lombard CM, Duncan SR, Rizk NW, Colby TV. The diagnosis of Wegener's granulomatosis from transbronchial biopsy specimens. Hum Pathol 1990;21:838–842.
32. Guinee DG Jr, Feuerstein I, Koss MN, Travis WD. Pulmonary lymphangioleiomyomatosis. Diagnosis based on results of transbronchial biopsy and immunohistochemical studies and correlation with high-resolution computed tomography findings. Arch Pathol Lab Med 1994;118: 846–849.
33. Churg A. Lung biopsy: handling and diagnostic limitations. In: Thurlbeck WM, ed. Pathology of the lung. Stuttgart: Thieme, 1988:67–78.
34. Churg A. Transbronchial biopsy. Nothing to fear. Am J Surg Pathol 2001;25:820–822.
35. Katzenstein A-L A, Askin FB. Interpretation and significance of pathologic findings in transbronchial lung biopsy. Am J Surg Pathol 1980;4:223–234.
36. Levin DC, Wicks AB, Ellis JH Jr. Transbronchial lung biopsy via the fiberoptic bronchoscope. Am Rev Respir Dis 1974;110:4–12.
37. Smith CW, Murray GF, Wilcox BR. The role of transbronchial lung biopsy in diffuse pulmonary disease. Ann Thorac Surg 1977;24:54–58.
38. Wall CP, Gaensler EA, Carrington CB, Hayes JA. Comparison of transbronchial and open lung biopsies in chronic infiltrative lung diseases. Am Rev Respir Dis 1981;123: 280–285.
39. Joyner LR, Schneinhorn DJ. Transbronchial forceps lung biopsy through the fiberoptic bronchoscope. Diagnosis of diffuse pulmonary disease. Chest 1975;67:532–535.
40. Poe RH, Utell MJ, Israel RH, Hall WJ, Eshleman JD. Sensitivity and specificity of the nonspecific transbronchial lung biopsy. Am Rev Respir Dis 1979;119:25–31.
41. Wilson RK, Fechner RE, Greenberg SD, Estrada R, Stevens PM. Clinical implications of a nonspecific transbronchial biopsy. Am J Med 1978;65:252–256.
42. Feldman NT, Pennington JE, Ehrie MG. Transbronchial lung biopsy in the compromised host. JAMA 1977;283: 1377–1379.
43. Matthay RA, Farmer WC, Odero D. Diagnostic fiberoptic bronchoscopy in the immunosuppressed host with pulmonary infiltrates. Thorax 1977;32:539–545.
44. Cunningham JH, Zavala DC, Corry RJ, Keim LW. Trephine air drill, bronchial brush and fiberoptic transbronchial lung biopsies in immunosuppressed patients. Am Rev Respir Dis 1977;115:213–220.
45. Lauver GL, Hasan FM, Morgan RB, Campbell SC. The usefulness of fiberoptic bronchoscopy in evaluating new pulmonary lesions in the compromised host. Am J Med 1979;66:580–585.
46. Phillips MJ, Knight RK, Green M. Fibreoptic bronchoscopy and diagnosis of pulmonary lesions in lymphoma and leukemia. Thorax 1980;35:19–25.
47. Puska S, Hutcheon MA, Hyland RH. Usefulness of transbronchial biopsy in immunosuppressed patients with pulmonary infiltrates. Thorax 1983;38:146–150.
48. Williams B, Yungbluth M, Adams G, Glassroth J. The role of fiberoptic bronchoscopy in the evaluation of immunocompromised hosts with diffuse pulmonary infiltrates. Am Rev Respir Dis 1985;131:880–885.

49. Jain P, Sundur S, Meli Y, Arroliga AC, Stoller JK, Mehta AC. Role of flexible bronchoscopy in immunocompromised patients with lung infiltrates. Chest 2004;125:712–722.
50. Chopra SK, Mohsenifar Z. Fiberoptic bronchoscopy in diagnosis of opportunistic infections: assessment of sputa, washings, brushings and biopsy specimens. West J Med 1979;131:4–7.
51. Pennington JE, Feldman NT. Pulmonary infiltrates and fever in patients with hematologic malignancy: Assessment of transbronchial biopsy. Am J Med 1977;62:581–587.
52. Anders GT, Linville KC, Johnson JE, Blanton HM. Evaluation of the float sign for determining adequacy of specimens obtained with transbronchial biopsy. Am Rev Respir Dis 1991;144:1406–1407.
53. Curley FJ, Johal JS, Burke ME, Fraire AE. Transbronchial lung biopsy. Can specimen quality be predicted at the time of biopsy? Chest 1998;113:1037–1041.
54. Fechner RE, Greenberg SD, Wilson RK, Stevens PM. Evaluation of transbronchial biopsy of the lung. Am J Clin Pathol 1977;68:17–20.
55. Fraire AE, Cooper SP, Greenberg SD, Rowland LP, Langston C. Transbronchial lung biopsy. Histopathologic and morphometric assessment of diagnostic utility. Chest 1992;102;748–752.
56. Shure D, Abraham JL, Konopka R. How should transbronchial biopsies be performed and processed? Am Rev Respir Dis 1982;126:342–343.
57. Attanoos R. Pitfalls in pulmonary pathology. Curr Diagn Pathol 2005;11:44–51.
58. Kendall DM, Gal AA. Interpretation of tissue artifacts in transbronchial lung biopsy specimens. Ann Diagn Pathol 2003;7:20–24.
59. Farrell DJ, Thompson PJ, Morley AR. Tissue artifacts caused by sponges. J Clin Pathol 1992;45:923–924.
60. Landas SK, Bromley CM. Sponge artifact in biopsy specimens. Arch Pathol Lab Med 1990;114:1285–1287.
61. Kepes JJ, Oswald O. Tissue artifacts caused by sponge in embedding cassettes. Am J Surg Pathol 1991;15:810–812.
62. Wang KP, Terry P, Marsh B. Bronchoscopic needle aspiration biopsy of paratracheal tumors. Am Rev Respir Dis 1978;118:17–21.
63. Wang KP, Marsh BR, Summer WR, Terry PB, Erozan YS, Baker RR. Transbronchial needle aspiration for diagnosis of lung cancer. Chest 1981;80:48–50.
64. Shure D, Fedullo PF. Transbronchial needle aspiration in the diagnosis of submucosal and peribronchial bronchogenic carcinoma. Chest 1985;88:49–51.
65. Gay PC, Brutinel WM. Transbronchial needle aspiration in the practice of bronchoscopy. Mayo Clin Proc 1989;64: 158–162.
66. Wang KP, Kaponik EF, Briff EJ, Khouri N, Erozan Y. Transbronchial needle aspiration of peripheral pulmonary nodules. Chest 1984;86:819–823.
67. Wang KP, Fishman EK, Britt EJ, Siegelman SS, Haponik EF, Erozan YS. Rigid transbronchial needle aspiration biopsy for histological specimens. Ann Otol Rhinol Laryngol 1985;94:382–385.
68. Mehta AC, Kavuru MS, Meeker DP, Gephardt GN, Nunez C. Transbronchial needle aspiration for histology specimens. Chest 1989;96:1228–1232.
69. Trisolini R, Agli LL, Cancellieri A, et al. The value of flexible transbronchial needle aspiration in the diagnosis of stage I sarcoidosis. Chest 2003;124:2126–2130.
70. Westcott JL. Percutaneous transthoracic needle biopsy. Radiology 1988;169:593–601.
71. Silverman I. A new biopsy needle. Am J Surg 1938;40: 671–672.
72. King EG, Bachynski JE, Mielke B. Percutaneous trephine lung biopsy. Evolving role. Chest 1976;70:212–216.
73. Steel SJ, Winstanley DP. Trephine biopsy of the lung and pleura. Thorax 1969;24:576–584.
74. Zavala DC, Bedell GN. Percutaneous lung biopsy with a cutting needle. An analysis of 40 cases and comparison with other biopsy techniques. Am Rev Respir Dis 1972; 106:186–193.
75. Balslor S, Vestbo J, Viskum K. Value of Tru-cut lung biopsy in focal and diffuse lung disease. Thorax 1988;43:147–150.
76. Meyer JE, Ferracci JT Jr, Janower ML. Fatal complications of percutaneous lung biopsy. Review of the literature and report of a case. Radiology 1970;96:47–48.
77. Moore EH. Technical aspects of needle aspiration lung biopsy: A personal perspective. Radiology 1998;208:303–318.
78. Manhire A, Charig M, Clelland C, et al. Guidelines for radiologically guided lung biopsy. Thorax 2003;58:920–936.
79. Greene R, Szyfelbein WM, Isler RJ, Stark P, Jantsch H. Supplementary tissue-core histology from fine-needle transthoracic aspiration biopsy. AJR 1985;44:787–792.
80. Yamagami T, Iida S, Kato T, et al. Usefulness of new automated cutting needle for tissue-core biopsy of lung nodules under CT fluoroscopic guidance. Chest 2003;124: 147–154.
81. Lucidarme O, Howarth N, Finet JF, Grenier PA. Intrapulmonary lesions: percutaneous automated biopsy with a detachable, 18-gauge, coaxial cutting needle. Radiology 1998;207:759–765.
82. Patz EFJr, Fidler J, Knelson M, Paine S, Goodman P. Significance of percutaneous needle biopsy in patients with multiple pulmonary nodules and a single known primary malignancy. Chest 1995;107:601–604.
83. Yamagami T, Iida S, Kato T, Tanaka O, Nishimura T. Combining fine-needle aspiration and core biopsy under CT fluoroscopy guidance: a better way to treat patients with lung nodules? AJR 2003;180:811–815.
84. Mitruka S, Landreneau RJ, Mack MJ, et al. Diagnosing the indeterminate pulmonary nodule: percutaneous biopsy versus thoracoscopy. Surgery 1995;118:676–684.
85. Klassen KP, Anlyan AJ, Curtis GM. Biopsy of diffuse pulmonary lesions. Arch Surg 1949;59:694–704.
86. Klassen KP, Andrews NC. Biopsy of diffuse pulmonary lesions: a seventeen-year experience. Ann Thorac Surg 1967; 4:117–124.
87. Chamberlain JM. Discussion of presentation on "mediastinoscopy." J Thorac Cardiovasc Surg 1965;49:20.
88. Robicsek F. Supraclavicular lung biopsy. J Thoracic Cardiovasc Surg 1995;110:1765–1766.
89. Jacobaeus HC. The practical importance of thoracoscopy in surgery of the chest. Surg Gynecol Obstet 1922;34:289–296.

90. Douglas JM, Jr. Thoracoscopic surgery. In: Sabistan DC Jr, Spencer FC, eds. Surgery of the chest. 6th ed. Philadelphia: WB Saunders, 1995:2149–2154.
91. Ferguson MK. Thoracoscopy for diagnosis of diffuse lung disease. Ann Thorac Surg 1993;56:694–696.
92. Carnochan FM, Walker WS, Cameron EW. Efficacy of video assisted thoracoscopic lung biopsy: an historical comparison with open lung biopsy. Thorax 1994;49:361–363.
93. Bensard DD, McIntyre RC Jr, Waring BJ, Simon JS. Comparison of videothoracoscopic lung biopsy to open lung biopsy in the diagnosis of interstitial lung disease. Chest 1993;103:765–770.
94. Krasna MJ, White CS, Aisner SC, Templeton PA, McLaughlin JS. The role of thoracoscopy in the diagnosis of interstitial lung disease. Ann Thorac Surg 1995;59:348–351.
95. Ginsberg MS, Griff SK, Go BD, Yoo HH, Schwartz LH, Panicek DM. Pulmonary nodules resected at video assisted thoracoscopic surgery. Etiology in 426 patients. Radiology 1999;213:277–282.
96. Langenfield JE. A new thoracoscopic lung biopsy clamp simplifies excision of pulmonary nodules. Ann Thorac Surg 2003;76:307–8.
97. Shrager JB, Kaiser LR. Thoracoscopic lung biopsy. Five commonly asked questions about video-assisted thoracic surgery. Postgrad Med 1999;106:139–152.
98. Landreneau RJ, Hazelrigg SR, Ferson PF, et al. Thoracoscopic resection of 85 pulmonary lesions. Ann Thorac Surg 1992;54:415–420.
99. Ferson PF, Landreneau RJ, Dowling RD, et al. Comparison of open versus thoracoscopic lung biopsy for diffuse infiltrative pulmonary disease. J Thorac Cardiovasc Surg 1993; 106:194–199.
100. Zegdi R, Azorin J, Tremblay B, Destable M, Lajos PS, Valeyre D. Videothoracoscopic lung biopsy in diffuse infiltrative lung diseases: a 5–year surgical experience. Ann Thorac Surg 1998;66:1170–1173.
101. Kadokura M, Colby TV, Myers JL, et al. Pathological comparison of video-assisted thoracic surgical lung biopsy with traditional open lung biopsy. J Thorac Cardiovasc Surgery 1995;109:494–498.
102. Gaensler EA, Ball-Moister MV, Hamm J. Open lung biopsy in diffuse pulmonary disease. N Engl J Med 1964; 270:1319–1331.
103. Gaensler EA, Carrington CB. Open lung biopsy for chronic diffuse infiltrative lung disease: clinical, roentgenographic and physiological correlations in 502 patients. Ann Thorac Surg 1980;30:411–426.
104. Scadding JG. Lung biopsy in the diagnosis of diffuse lung disease. Br Med J 1970;2:557–564.
105. Ray JF III, Lawton BR, Myers WO, et al. Open pulmonary biopsy: 19 years experience with 416 consecutive operations. Chest 1976;69:43–47.
106. Newman SL, Michel RP, Wang NS. Lingular lung biopsy: Is it representative? Am Rev Respir Dis 1985;132:1084–1086.
107. Wetstein L. Sensitivity and specificity of lingular segmental biopsies of the lung. Chest 1986;90:383–386.
108. Miller RR, Nelems B, Muller NL, Evans KG, Ostrow DN. Lingular and right middle lobe biopsy in the assessment of diffuse lung disease. Ann Thorac Surg 1987;44:269–272.
109. Churg A. An inflation procedure for open lung biopsies. Am J Surg Pathol 1983;7:69–71.
110. Wilson WR, Cockerill FR III, Rosenow EC III. Pulmonary disease in the immunocompromised host. Mayo Clin Proc 1985;60:610–63.
111. Rosenow EC, III, Wilson WR, Cockerill FR III. Pulmonary disease in the immunocompromised host. (first of two parts). Mayo Clin Proc 1985;60:473–487.
112. Dail DH. Introduction to AIDS pathology. In: Dail DH, Hammar SP, eds. Pulmonary pathology. 2nd ed. New York: Springer-Verlag, 1993:121–155.
113. Roback SA, Weintraub WH, Nesbit M, Spanos PK, Burke B, Leonard AS. Diagnostic open lung biopsy in the critically ill child. Pediatrics 1973;52:605–608.
114. Greenman RL, Goodall PT, King D. Lung biopsy in immunocompromised hosts. Am J Med 1975;59:488–496.
115. Rosen PP, Martini N, Armstrong D. *Pneumocystis carinii* pneumonia: diagnosis by lung biopsy. Am J Med 1975;58: 794–802.
116. Nelems JM, Cooper JD, Henderson RD, Peng T, Phillips MJ. Emergency open lung biopsy. Ann Thorac Surg 1976; 22:260–263.
117. Wolff U, Bartlett M, Baehner RL, Grosfeld JL, Smith JW. The causes of interstitial pneumonia in immunocompromised children. An aggressive systemic approach to diagnosis. Pediatrics 1977;60:41–45.
118. Leight GS Jr, Michaelis LL. Open lung biopsy for the diagnosis of acute, diffuse pulmonary infiltrates in the immunosuppressed patient. Chest 1978;73:477–482.
119. Singer C, Armstrong D, Rosen PP, Walzer PD, Yu B. Diffuse pulmonary infiltrates in immunosuppressed patients: Prospective study of 80 cases. Am J Med 1979;66:110–120.
120. Rossiter SJ, Miller C, Churg AM, Carrington CB, Mark JBD. Open lung biopsy in the immunosuppressed patient: Is it really beneficial? J Thorac Cardiovasc Surg 1979;77: 338–345.
121. Toledo-Pereyra LH, DeMeester TR, Kinealey A, MacMahon H, Churg A, Golomb H. The benefits of open lung biopsy in patients with previous non-diagnostic transbronchial lung biopsy: A guide to appropriate therapy. Chest 1980;77:647–650.
122. Tenholder MF, Hooper RG. Pulmonary infiltrates in leukemia. Chest 1980;78:468–473.
123. Waltzer WC, Sterioff S, Zincke H, Bernetz PE, Brewer NS. Open lung biopsy in the renal transplant recipient. Surgery 1980;88:601–610.
124. Jaffee JP, Maki DG. Lung biopsy in immunocompromised patients: one institution's experience and an approach to management of pulmonary disease in the compromised host. Cancer 1981;48:1144–1153.
125. Hiatt JR, Gong H, Mulder DG, Ramming KP. The value of open lung biopsy in the immunosuppressed patient. Surgery 1982;92:285–291.
126. Canham EM, Kennedy TC, Merrick TA. Unexplained pulmonary infiltrates in the compromised patient: an invasive investigation in a consecutive series. Cancer 1983;52:325–329.
127. McKenna RJ Jr, Mountain CF, McMurtry MJ. Open lung biopsy in immunocompromised patients. Chest 1984;86: 671–674.

128. Prober CG, Whyte H, Smith CR. Open lung biopsy in immunocompromised children with pulmonary infiltrates. Am J Dis Child 1984;138:60–63.
129. McCabe RE, Brooks RG, Mark JBD, Remington JS. Open lung biopsy in patients with acute leukemia. Am J Med 1985;78:609–616.
130. Cockerill FR, III, Wilson WR, Carpenter HA, Smith TF, Rosenow EC III. Open lung biopsy in immunocompromised patients. Arch Intern Med 1985;145:1398–1404.
131. Robin ED, Burke EM. Lung biopsy in immunosuppressed patients. Chest 1986;89:276–278.
132. Kramer MR, Berkman N, Mintz B, Godfrey S, Saute M, Amir G. The role of open lung biopsy in the management of patients with diffuse lung disease. Ann Thorac Surg 1998;65:198–202.
133. Neff TA. Lung biopsy: How vs. whom? Chest 1976;70: 201–202.
134. Neuhaus SJ, Matar KS. The efficacy of open lung biopsy. Aust NZ J Surg 1997;67:181–184.
135. LoCicero J. Does every patient with enigmatic lung disease deserve a lung biopsy. The continuing dilemma. Chest 1994;106:706–708.
136. Epler GR, McLoud TC, Gaensler EA, Mikus JP, Carrington CB. Normal chest roentgenograms in chronic diffuse infiltrative lung disease. N Engl J Med 1978;298: 934–939.
137. Temes R, Joste NE, Qualls CR, et al. Lung biopsy: Is it necessary? J Thorac Cardiovasc Surgery 1999;118:1097–1100.
138. Colby TV, Yousem SA. Lungs. In: Sternberg SS, ed. Histology for pathologists. New York: Raven Press, 1992:479–497.
139. Yazdy AM, Chung-Park M, Supinski G. Restrictive ventilatory defect associated with pulmonary hypertension in mixed connective tissue disease. J Rheumatol 1990;17: 121–123.
140. Sils B. A multidisciplinary method for study of lung structure and function. Am Rev Respir Dis 1962;86:238–245.
141. Mark EJ. The second diagnosis: the role of the pathologist in identifying pneumoconioses in lungs excised for tumors. Hum Pathol 1981;12:585–587.
142. Gibbs AR, Seal RME. Examination of lung specimens. J Clin Pathol 1990;43:68–72.
143. Ludwig J. Tracheobronchial tree and lungs. In: Ludwig J, ed. Handbook of autopsy practice. 3rd ed. Totowa, NJ: Humana Press, 2002:45–52.
144. Start RD, Cross SS. Pathological investigation of deaths following surgery, anaesthesia, and medical procedures. J Clin Pathol 1999;52:640–652.
145. Fraser RS. Lung perforation complicating tube thoracotomy: pathologic description of three cases. Hum Pathol 1988;19:518–523.
146. Fraser RS. Catheter-induced pulmonary artery perforation: pathologic and pathogenic features. Hum Pathol 1987; 18:1246–1251.
147. Craighead JE, Abraham JL, Churg A, et al. The pathology of asbestos-associated diseases of the lungs and pleural cavities: diagnostic criteria and proposed grading schema. Arch Pathol Lab Med 1982;106:543–596.
148. Whimster WE. Techniques for the examination of excised lungs. Hum Pathol 1970;1:305–314.
149. Weibel EF. Morphometry of the human lung. Berlin: Springer-Verlag, 1963:48–50.
150. Dunnill MS, Fletcher CM, Cumming G, et al. Quantitative assessment of chronic non-specific lung disease at necropsy. Thorax 1975;30:241–251.
151. Gough J, Wentworth JE. The use of thin sections of entire organs in morbid anatomical studies. J R Microsc Soc 1949;69:231–235.
152. Whimster WF. Rapid giant paper sections of lungs. Thorax 1969;24:737–741.
153. Heard BE. A pathological study of emphysema of the lungs with chronic bronchitis. Thorax 1958;13:136–149.
154. Heard BE. Pathology of pulmonary emphysema: Methods of study. Am Rev Respir Dis 1960;82:792–799.
155. Hislop A, Reid L. Pulmonary arterial development during childhood; branching pattern and structure. Thorax 1973; 28:129–135.
156. Reid L. The lung: Its growth and remodeling in health and disease. AJR 1977;129:777–788.
157. Lauweryns JM. The blood and lymphatic microcirculation of the lung. Pathol Annu 1971;6:365–415.
158. Liebow AA, Hales MR, Lindskog GE, Bloomer WE. Plastic demonstrations of pulmonary pathology. Bull Int Assoc Med Museums 1947;27:116–129.
159. Timbrell V, Bevan NE, Davies AS, Munday DE. Hollow casts of lungs for experimental purposes. Nature 1970;225: 97–98.
160. Eisman MM. Lung models: hollow, flexible reproductions. J Appl Physiol 1970;29:531–533.
161. Whitwell E. A study of the pathology and pathogenesis of bronchiectasis. Thorax 1952;7:213–239.
162. Heard BE, Esterly JR, Wootliff JS. A modified apparatus for fixing lungs to study the pathology of emphysema. Am Rev Respir Dis 1967;95:311–312.
163. Blumenthal BJ, Boren HG. Lung structure in three dimensions after inflation and fume fixation. Am Rev Tuberc 1959;79:764–772.
164. Markarian B. A simple method of inflation-fixation and air-drying of lungs. Am J Clin Pathol 1975;63:20–24.
165. Pratt PC. Preparation of normal and emphysematous lung tissue for structural study of bronchioles, alveolar ducts, and alveoli. Am Rev Tuberc 1959;79:842–843.
166. Wright BM, Slavin G, Kreel L, Callan K, Sandin B. Postmortem inflation and fixation of human lungs. A technique for pathological and radiological correlations. Thorax 1974; 29:189–194.
167. Weibel ER ,Vidone RA. Fixation of the lung by formalin steam in a controlled state of air inflation. Am Rev Respir Dis 1961;84:856–861.
168. Pratt PC, Klugh GA. A technique for the study of ventilatory capacity, compliance and residual volume of excised lungs and for fixation, drying, and serial sectioning in the inflated state. Am Rev Respir Dis 1961;83:690–696.
169. Landing BH, Wells TR. Tracheobronchial anomalies in children. Perspect Pediatr Pathol 1973;1:1–32.
170. Davis S, Bove KE, Wells TR, Hartsell B, Weinberg A, Gilbert E. Tracheal cartilaginous sleeve. Pediatr Pathol 1992;12:349–364.
171. Stovin PGI. Congenital lobar emphysema. Thorax 1959;14: 254–262.

172. Tandon MK, Campbell AH. Bronchial cartilage in chronic bronchitis. Thorax 1969;24:607–612.
173. Thurlbeck WM, Pun R, Toth J, Frazer RG. Bronchial cartilage in chronic obstructive lung disease. Am Rev of Respir Dis 1974;109:73–80.
174. Fulton RM, Hutchinson EC, Jones AM. Ventricular weight in cardiac hypertrophy. Br Heart J 1952;14:413–421.
175. Hislop A, Reid L. Weight of the left and right ventricle of the heart during fetal life. J Clin Pathol 1972;25:534–536.

2
Anatomy and Histology of the Lung

Joseph F. Tomashefski, Jr., and Carol F. Farver

The lung is uniquely designed to accomplish its major functions of movement of air and the delivery of oxygen to and removal of carbon dioxide from the circulation. Pulmonary anatomic compartments are tightly integrated for this purpose, while redundancy of structures and provisions for collateral ventilation and blood flow enable the lung to rapidly adjust to physiologic demands and meet the challenges imposed by disease. The intricate net-like connective tissue skeleton of the lung, with its intrinsic elasticity, enables the lung to function as a cohesive unit. Protected by the rigid thoracic cage and sealed in a bellows-like chamber, the lung responds to cyclical volume and pressure fluctuations coordinated with contractions of the diaphragm and thoracic muscles of respiration on the order of 16 breaths per minute.

Espousing the precept that an understanding of normal anatomy is essential for the recognition and appreciation of abnormal structure, this chapter on practical lung anatomy and histology provides the reader with a baseline for the evaluation of macroscopic, histologic, and ultrastructural changes imparted by disease. A working conception of regional lung anatomy at the gross and microscopic level is also essential for the accurate localization of lesions. For this purpose, fixation of the lung in the inflated state is optimal (see Chapter 1). Knowledge of normal lung structure is also crucial for understanding radiologic appearances and in making radiographic correlations, which have become an important adjunct in the assessment of lung biopsy samples.[1,2]

Perhaps more than any other organ, the lung lends itself to anatomic and physiologic correlations. With the normal anatomy as a starting point, the pulmonary pathologist is in an ideal position to develop an appreciation of the way in which abnormal structure is reflected in deviant function. Excellent texts that correlate anatomy with respiratory physiology and pulmonary function tests are those by Bates and colleagues[3] and Fishman and colleagues.[4] Special morphologic techniques used in the study of the lung are presented in Chapter 1. The quantitative expression of lung anatomy and its morphometric evaluation are discussed by Weibel and Taylor.[5]

External Features

The right and left lungs, invested in the visceral pleura, reside in their respective hemithoracic cavities, separated by the heart and mediastinal structures and bordered inferiorly by the diaphragm. Because the size of the lung is dependent on its volume, lung weight is the usual measurement provided in anatomic descriptions. The normal weight range of each lung in an adult is roughly 300 to 450 g.[6] Increased lung weight is an indication of congestion, edema, or inflammatory exudates. Lung volume, measured in the inflated state by water displacement, ranges from 3.5 to 8.5 L for both lungs.[6,7] The right lung is slightly larger than the left by a volume ratio of 53% to 47%.[6] Due to their elastic nature, the lungs shrink to approximately one-third their size when the thoracic cavity is opened.[8]

The lung is covered by a smooth glistening visceral pleura. The pleural membrane is translucent, but as it rests on the lung, the visceral pleural surface appears pink. With increasing age, the pleura invariably accumulates black pigment, the amount of which is a reflection of the degree of exposure to environmental particulates. Pigment tends to deposit in a reticular fashion along the pleural lymphatics and is usually accentuated in the upper lobe. Interesting patterns of pigmentation include linear deposition at the angles of the lobes, or accentuation along the rib indentations (Fig. 2.1). Nodular accumulation of pigment is associated with subpleural lymphoid aggregates. Gray thickening indicates pleural fibrosis that is frequently seen at the lung apex as the "apical fibrous cap" (see Fig. 30.10 in Chapter 30).[9] The visceral pleura wraps around the lung and is reflected from the mediastinal pleura at the hilum and pulmonary ligament. Prominent pleural indentations include, on the right, grooves for the esophagus and supe-

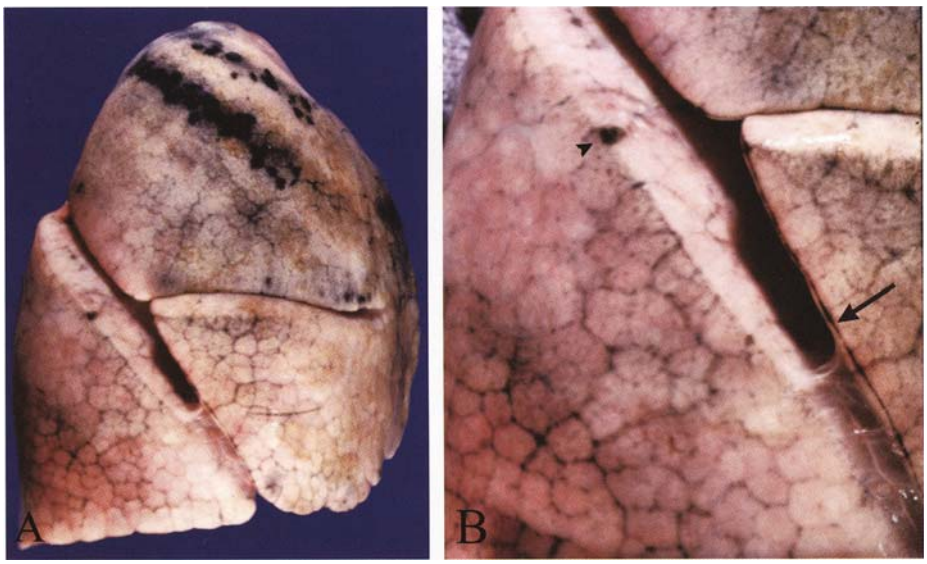

FIGURE 2.1. **A.** Lateral external view of right lung. The horizontal fissure is incomplete anteriorly. Black pigment is accentuated in the upper lobe, following the indentations of the ribs. **B.** Pigment outlines the pleural lymphatics, which demarcate the boundaries of secondary lobules. A pigmented nodule is seen in the lower lobe (arrowhead). Note also the linear deposit of pigment (arrow) along the inferior angle of the middle lobe.

rior vena cava, and a cardiac impression. On the left side the cardiac impression is more pronounced and there is an indentation (the cardiac notch) in the area of the lingula. A prominent crook-shaped aortic groove is located superiorly and posteriorly to the left hilum.[10]

Lobes and Fissures

The right lung is divided into three lobes—upper, middle, and lower—that are demarcated from one another by a diagonal (major) fissure that separates the lower from the upper and middle lobes, and a horizontal (minor) fissure that separates the middle from the upper lobe (Fig. 2.1).[11] The left lung is composed of an upper and lower lobe separated by a single diagonal fissure. The lingula *(L. tongue),* which represents the anterior–inferior division of the left upper lobe, overrides the left cardiac ventricle, and is the counterpart of the right middle lobe. Although readily accessible by a mini-thoracotomy, routine biopsy of the lingula for diffuse pulmonary disease has been discouraged because the lingula, like the right middle lobe, frequently has old pathologic or nonspecific changes not necessarily related to the current disease process (see Chapter 1).[12]

Deviations in fissure anatomy and distribution, including accessory and partial fissures, are common.[13] Usually the anterior aspect of the horizontal fissure is incomplete, potentially allowing for collateral ventilation between the right upper and middle lobes (Fig. 2.1). Occasionally a horizontal fissure separates the lingula from the rest of the left upper lobe forming a trilobed left lung (pseudo–right lung). Conversely, absence of the horizontal fissure produces a bilobate right lung. Any segment of the lung may be partially or completely segregated by an accessory (supernumerary) fissure, a relatively frequent anomaly occurring in up to 50% of specimens.[1,13] Common accessory fissures include the inferior accessory fissure of the right lower lobe, which isolates the medial basal segment as the retrocardiac lobe (Fig. 2.2), and an accessory fissure separating the superior segment ("dorsal lobe") from the lower lobe basal segments, also said to be more common on the right.[1,13] From a practical standpoint, deviations in fissure formation are of greatest

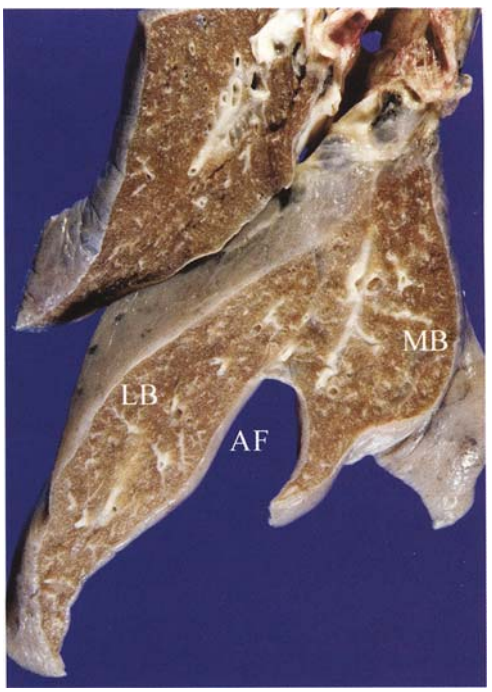

FIGURE 2.2. Accessory fissure (AF) separating medial basal (MB) segment from the other basal segments of the right lung. LB, lateral basal segment.

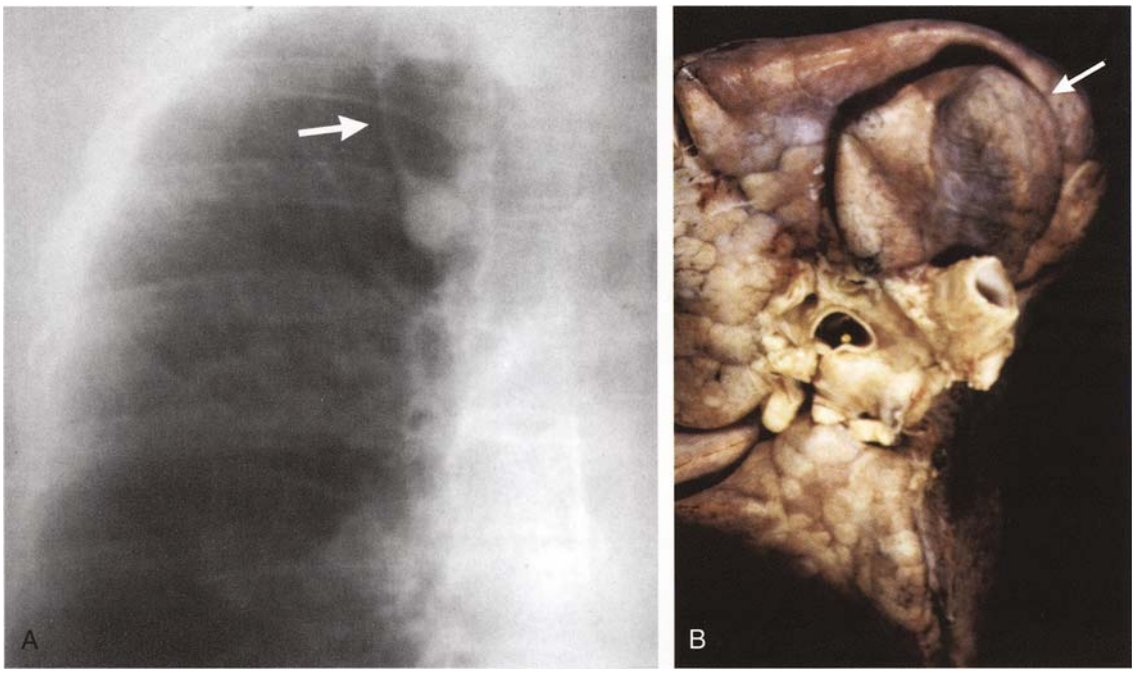

FIGURE 2.3. Azygos lobe. **A.** Azygos fissure (arrow) in the medial aspect of the right upper lobe visualized in a posteroanterior (PA) chest x-ray. **B.** Medial view of right lung showing segregated azygos lobe (arrow) superior to the main bronchus. The posterior aspect of the specimen is to the right.

importance to the radiologist, and to the surgeon when planning a lung resection.

A particularly interesting anomalous fissure, the azygos fissure, is a vertically oriented cleft dividing the apical segment of the right upper lobe, seen in approximately 1% of anatomic specimens and 0.4% of chest radiographs.[14,15] It is thought to be produced by the downward invagination of the azygos vein with its pleural investment, thus forming a mesoazygous.[16] The segregated portion of lung is termed the azygos lobe (Fig. 2.3). The azygos fissure presents radiographically as an oblique line across the apical portion of the right upper lobe, terminating in a teardrop shadow that represents the azygos vein seen on end (Fig. 2.3A).[1,15] The bronchial and arterial supply of the azygos lobe arise from the apical or posterior segments of the right upper lobe.[16]

Bronchopulmonary Segments

For localization of lesions it is important to understand the anatomy of the bronchopulmonary segments. A segment refers to that portion of lung supplied by a segmental bronchus (see below).[17] Except in situations of aberrant fissures, bronchopulmonary segments do not have defined anatomic boundaries, and a pathologist must estimate the localization of a segment based on the supplying airway. The bronchopulmonary segments are listed in Table 2.1, and the usual segmental distribution of each lung is shown schematically in Figure 2.4. The terminology of the bronchopulmonary segments is that originally proposed by Jackson and Huber.[17] Compared to the right lung, the apical and posterior segments of the left upper lobe and the anterior and medial basal segments of the left lower lobe are often each supplied by a single bronchus, and are referred to as the apicoposterior and anteromedial basal segments, respectively. The lingula is composed of a superior and inferior segment as com-

TABLE 2.1. Lobes and segments of the lung

Right lung		Left lung	
Lobe	Segment	Lobe	Segment
Upper	Apical (1)*	Upper	Apical[a] (1)
	Posterior (2)		Posterior[a] (2)
	Anterior (3)		Anterior (3)
Middle	Lateral (4)	Lingular	Superior (4)
	Medial (5)		Inferior (5)
Lower	Superior (6)	Lower	Superior (6)
	Medial basal (7)		Medial basal[a] (7)
	Anterior basal (8)		Anterior basal[a] (8)
	Lateral basal (9)		Lateral basal (9)
	Posterior basal (10)		Posterior basal (10)

[a]The two segments are frequently fused and considered as a single segment.

*Numbers in parentheses refer to the numbering of segments in Fig. 2.4.

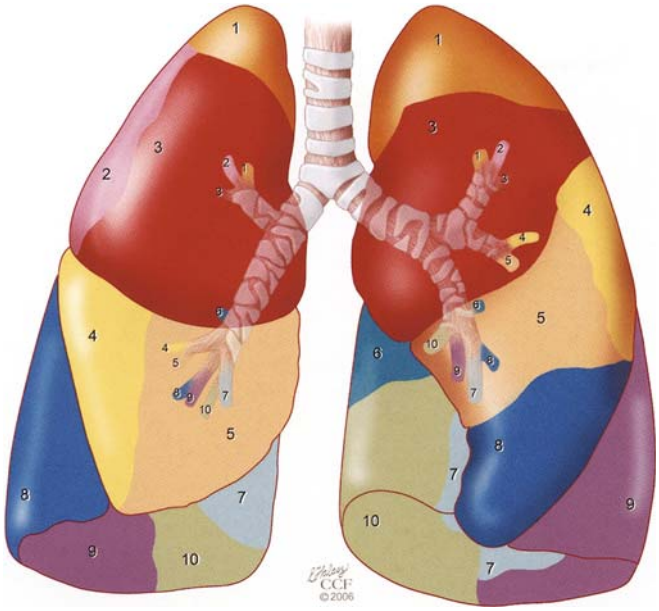

FIGURE 2.4. Schematic of the segmental anatomy of the lungs (see Table 2.1 for orientation and a key to the numbering). The right lower lobe superior segment (6) and the left upper lobe posterior segment (2) are not visualized from this anterior view.

pared to the medial and lateral segments of the right middle lobe.

Bronchi

Branching Pattern

Just below the level of the aortic arch, the tracheal carina marks the bifurcation of the right and left main bronchi. The left main bronchus angles 40 to 60 degrees off the original course of the trachea and extends longer than the right main bronchus as it circumvents the left side of the heart. The right main bronchus deviates only 20 to 30 degrees off the course of the trachea, following a nearly straight path into the right lower lobe bronchus. The straighter course of the right main bronchus predisposes to aspiration in the upright position (see Chapter 5).[12] The rigidity of the extrapulmonary bronchi is maintained by cartilaginous C-rings.

In the right hilum the main bronchus (Figs. 2.4 and 2.5) divides into the right upper lobe bronchus and a short segment, the bronchus intermedius, which then divides into the middle and lower lobe bronchi. The upper lobar bronchus divides into the three segmental bronchi. The middle lobe bronchus divides into the medial and lateral segmental bronchi. The right lower lobe bronchus is quite short due to the abrupt takeoff of the posteriorly directed lower lobe superior segmental bronchus at about the level of the middle lobe bronchial origin. The lower lobe bronchus then proceeds toward the more distal bifurcations of the four basal segmental bronchi (Fig. 2.4). The left main bronchus divides into upper and lower lobar branches. The left upper lobe bronchus branches into a superior division, which gives rise to apicoposterior and anterior segmental branches, and the inferior (lingular) division.[17] The lower lobe bronchus divides into the superior segmental bronchus (as on the right) and continues to the four basal segmental divisions.[6,17]

The bronchi accompany the pulmonary arteries as bronchovascular bundles surrounded by a connective tissue sheath. With each division the caliber of the airways narrows. The number of airway divisions varies among lobes. The axial pathway (from the main bronchus to the terminal bronchiole) may contain as many as 25 divisions or as few as five airway generations (along shorter pathways).[6] Normally bronchi are not macroscopically visible within 2 cm of the visceral pleura.

Connective Tissue, Cartilage, and Smooth Muscle

Connective tissue and smooth muscle provide the basic structure of the conducting airways. There are 16 to 20 tracheal cartilage rings, each of which is a C-ring that encircles approximately two thirds of the circumference of the trachea, leaving an opening on the posterior surface that allows for expansion of food boluses traveling within the adjacent esophagus. The rings are composed of hyaline cartilage that may calcify and ossify with age. The most proximal and distal cartilage rings of the trachea differ from the others. The first ring is bifurcated and attached

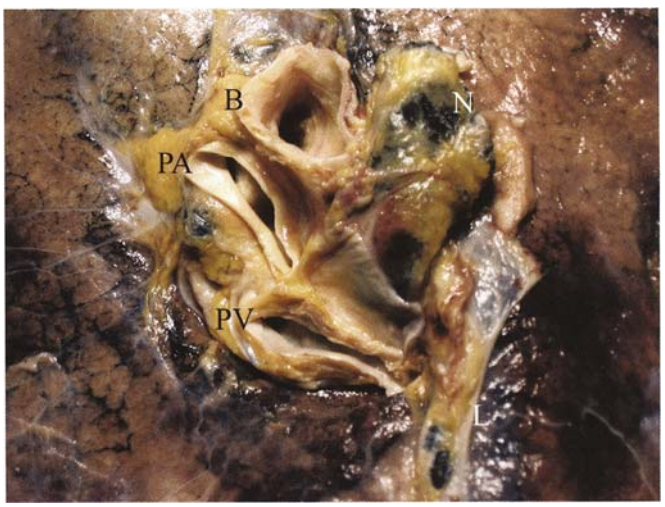

FIGURE 2.5. Hilar structures. Hilum of right lung showing relationship of main bronchus (B), pulmonary artery (PA) and vein (PV), hilar lymph node (N), and inferior pulmonary ligament (L). The anterior aspect of the specimen is to the left.

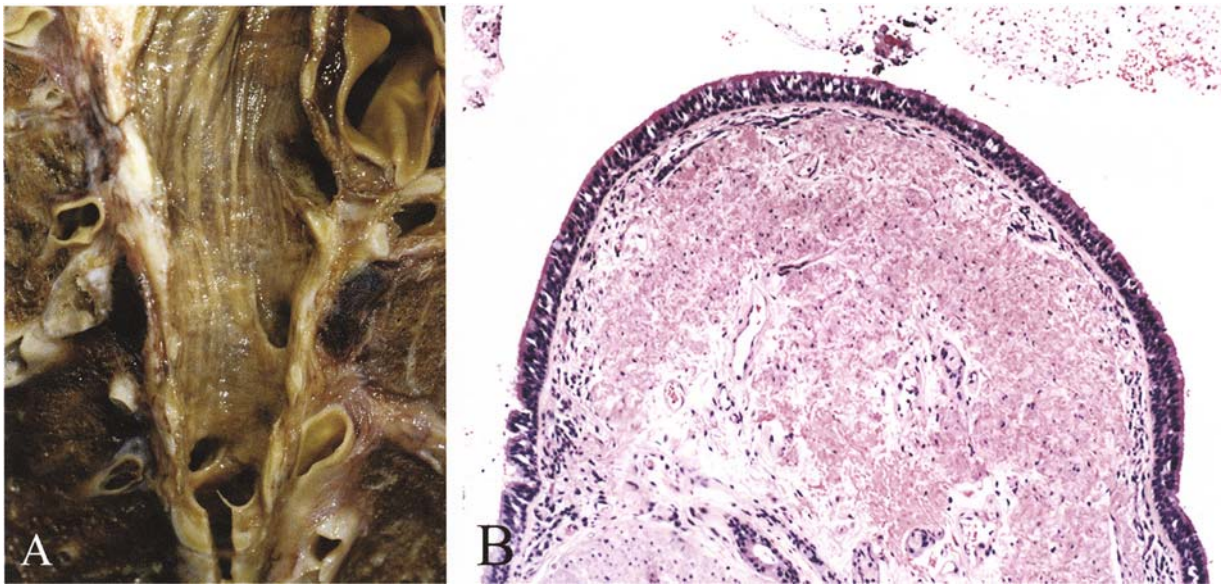

FIGURE 2.6. **A.** Longitudinally oriented elastic fibers create striations in the intrapulmonary bronchial mucosa. Note adjacent pulmonary arterial branches (bronchovascular bundles). **B.** Microscopic detail of submucosal elastic bundle in large bronchus.

to the cricoid cartilage of the larynx. The last tracheal cartilage is wider than the others with a triangular-shaped lower border with two semi–ring-shaped areas that give rise to the cartilages of the two major bronchi.[18] In between each cartilaginous ring and on the posterior surface of the trachea and main bronchi, is a fibrous membrane composed of collagen and elastic fibers, the latter of which provide for some recoil from stretching during breathing.

Beginning in the main bronchi just proximal to the lobar bronchi, the bronchial cartilage is organized circumferentially into haphazard irregular plates that decrease in size and areal density as the bronchi extend into the lung (Fig. 2.4; also see Fig. 1.12 in Chapter 1). With the rapid decrease in the cartilage mass, the circular smooth muscle bundles become the most prominent mural components in medium-sized bronchi, and it is here that bronchoconstriction is most efficient. A few fibers of longitudinal smooth muscle may be present, external to the circular smooth muscle. More peripherally, smooth muscle decreases in amount and becomes scarce in the terminal bronchiole. In chronic obstructive lung disease, smooth muscle proliferates centrifugally and can be found prominently even around the orifice of the alveolar duct. Elastic fibers run longitudinally in the larger bronchi (Fig. 2.6) and become helical toward the peripheral airways, like coiled metal springs, and then continue into the alveolar wall forming integrated fine networks. The outer limits of the extrapulmonary conducting airways are poorly defined. Alveolar walls form the outer limit of the intrapulmonary bronchi, bronchioles, and pulmonary arteries.

Bronchial Glands

Mucoserous glands are present in the submucosa of the trachea and bronchi. These submucosal glands contain both mucous cells and serous cells, both of which contribute to the secretions of the mucous bilayer covering the bronchial epithelium (Figs. 2.7 and 2.8). These mucinous secretions contain bacteriostatic lysozymes and lactoferrins, antibodies (immunoglobulin A, IgA) from the surrounding plasma cells, and some antiproteases. In older individuals glandular cells may be largely replaced by oxyphil cells (oxyphil metaplasia) (Fig. 2.8B). Approximately one opening of the duct of the bronchial gland can be found in a 1-mm-square area in large human bronchi. Ciliated cells usually extend into the duct for a short distance (Fig. 2.8C). The bronchial duct divides into one or more generations, depending on the size of the gland, before reaching the glandular acinus. Myoepithelial cells line the secretory parts of the glands and are controlled by the autonomic nervous system (Fig. 2.8D).

The volume of the bronchial glands is estimated by the gland-to-wall ratio (Reid index) or point-counting methods on random light microscopic sections of a major bronchus. The Reid index is calculated by measuring the thickness of the bronchial gland divided by the distance between the basal lamina of the bronchial mucosa and the nearest perichondrium (Fig. 2.7B). For this determination, a well-oriented bronchial cross section of a mainstem bronchus is necessary, and an average of several measurements is optimal. For a practical estimation of the mucous gland mass, an "eyeball" estimate may suffice.

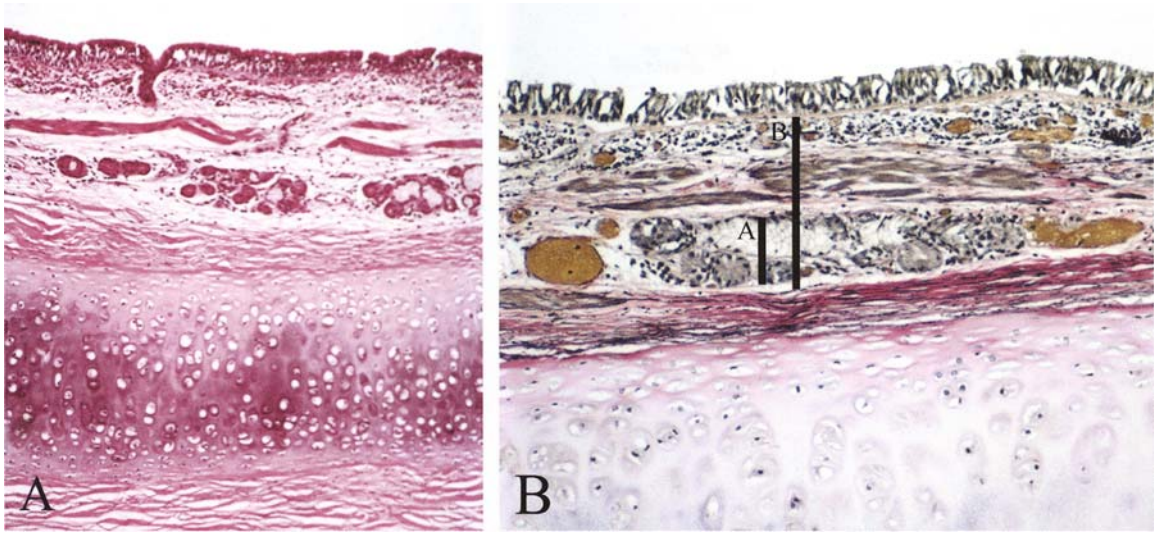

FIGURE 2.7. Bronchial wall. **A.** Low magnification of the bronchial wall for orientation. **B.** The Reid index is calculated as the percentage of line A divided by line B (see text). (Elastic van Gieson [EVG].)

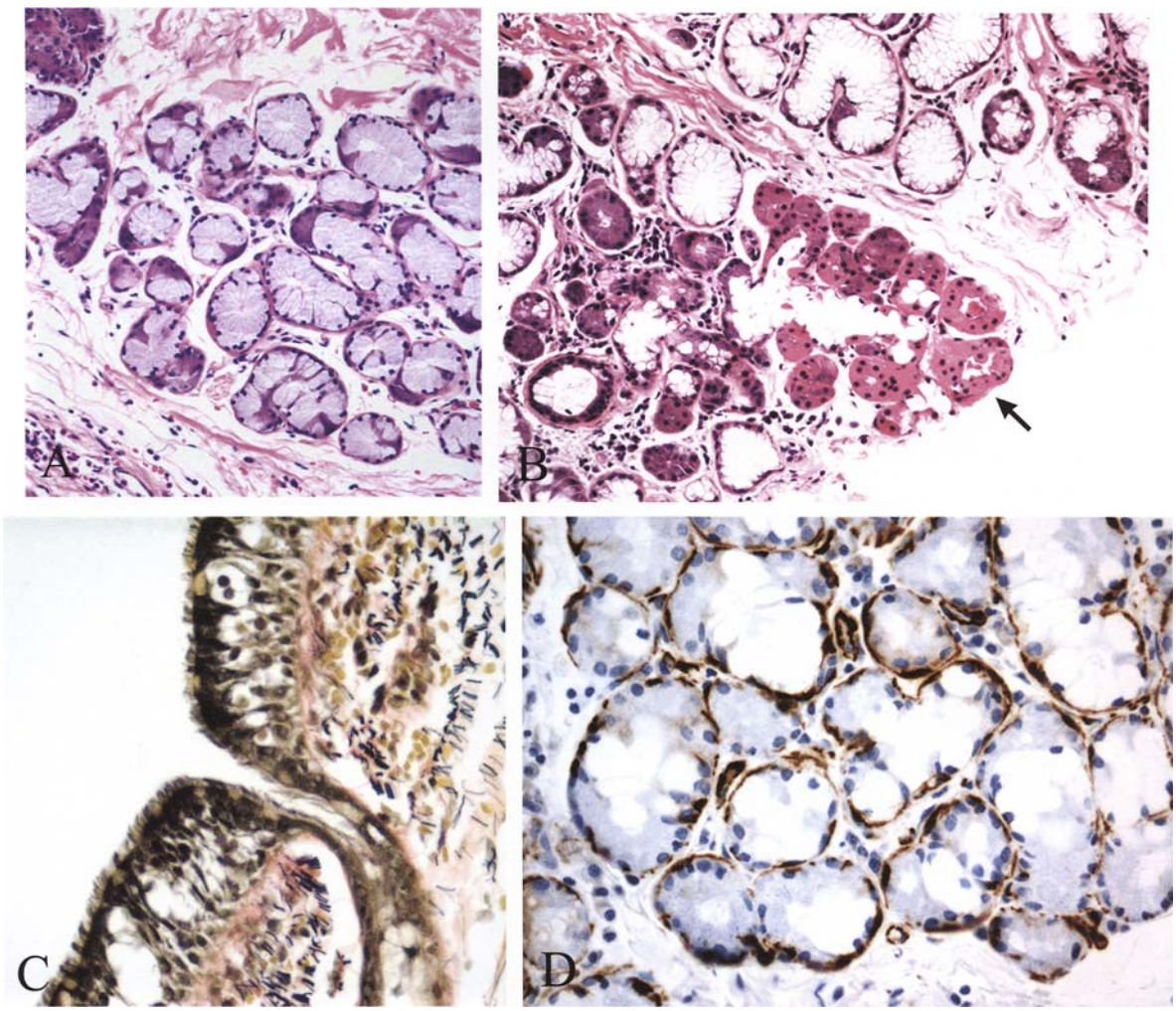

FIGURE 2.8. Seromucinous glands. **A.** Seromucinous gland. **B.** Oxyphil metaplasia involving a portion of the glandular lobule (arrow). **C.** High magnification of a ciliated intercalated duct. **D.** Actin filaments ensheath the mucous gland. (Immunohistochemical stain for muscle-specific actin.)

In patients without chronic bronchitis the Reid index is usually ≤0.4.[19,20]

Mucosa

The tracheal and bronchial mucosa is continuous with the larynx and consists of a pseudostratified ciliated columnar epithelium interspersed with goblet cells that sit on a basement membrane. The bronchial basement membrane is a thin layer of extracellular matrix that provides support for the epithelium. By light microscopy the bronchial basement membrane measures approximately 7 μm in thickness.[21] The major molecular constituents are collagen IV, fibronectin, laminin-entactin/nidogen complexes, and proteoglycans.[21–23] What appears as a homogeneous basement membrane by light microscopy, however, is actually a bilaminar structure consisting of the basal lamina (true basement membrane) and the deeper lamina reticularis. Thickening and fibrosis of the lamina reticularis is characteristic of bronchial asthma.

The four major types of cells that make up the epithelium are (1) ciliated cells, (2) goblet cells, (3) basal cells, and (4) neuroendocrine cells (Fig. 2.9). Layered atop the epithelium is the airway surface liquid[21] that, with the cilia, comprise the mucociliary escalator that traps foreign particles and organisms that enter the airways and propels them up and out of the conducting airways via the larynx.[24]

Ciliated Cells

The main function of the ciliated cells of the mucosa is to propel foreign particles/organisms via the mucociliary clearance mechanism. The number and importance of ciliated cells in the air passage are best illustrated by a scanning electron microscopic view of the surface of the large bronchus, where cilia appear to cover the entire surface (Fig. 2.10). The ciliated cell in the large bronchus is up to 20 μm in length and 10 μm in width, and contains about 200 cilia of 3 to 6 μm in length on the luminal surface. The nucleus is basal, and the cytoplasm is rich in mitochondria, which accumulate apically to supply energy for cilia (Fig. 2.11). The size of the cell and the length of the cilia decrease as the diameter of the bronchus decreases.

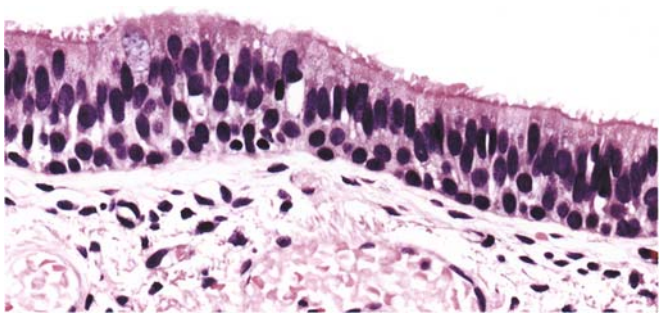

FIGURE 2.9. Light microscopic image of the bronchial mucosa showing the ciliated cells, rare goblet cells, and bronchial basal cells resting on a thin basement membrane.

A cilium has an intracytoplasmic basal body that is enmeshed and stabilized in place by a fibrillary network immediately beneath the cell membrane. From the basal body a long striated root extends and anchors deep into the cytoplasm, and a basal foot aligns itself sideward in the direction of the effective stroke of the cilium. At the neck, or the portion where the cilium emerges from the cell, the cell membrane forms a rosary-like modification called the necklace. The cilium tends to break off but also regenerates itself from this neck portion. The main body of the cilium is formed by an axoneme surrounded by the extension of cell membrane. The axoneme consists of a central pair and nine peripheral doublets of microtubules (see Fig. 5.41 in Chapter 5). Each doublet has a complete tubule (A subfiber) and an attached three-quarter circle of B subfiber. From the A subfiber, two rows of side arms (the inner and outer dynein arms) protrude toward the B subfiber of the adjacent doublet, and one radial spoke extends toward the central pair. The dynein arms are formed by protein with high adenosine triphosphatase (ATPase) activity. At the distal end of the cilium are hooking devices or bristles. (A detailed discussion of the ultrastructure and pathology of the cilia is provided in Chapter 5.)

The cilia extend into the overlying air surface liquid (ASL), which measures 5 to 100 μm in thickness. The ASL is a bilayer of a low-viscosity or watery (sol) lower layer (a product of the serous and mucous glands in the submucosa), and a high-viscosity or gel upper layer secreted from the goblet cells in the epithelium.[24] The cilia bend and beat back and forth by sliding opposing groups of doublets in opposite directions, which is accomplished by repeated attachments and detachments of dynein arms to adjacent doublets, similar to the motions used in jacking up a car. The recovery stroke of the ciliary beat is believed to be curved and to occur completely within the watery (sol) layer of the mucus. The effective stroke is done with cilia straight up, which allows the bristles to catch and propel forward the gel or viscous mucus on top of the sol layer to the larynx where it can be expectorated. The rate of the ciliary beat is usually 12 to 16 beats/second and metachronous[25] and is coordinated by intercellular gap junctions that allow for spread of this beat among the ciliated cells.

Cilia and ciliated cells are constantly exposed and vulnerable to many noxious agents including cigarette smoke. Therefore, ultrastructural ciliary changes are

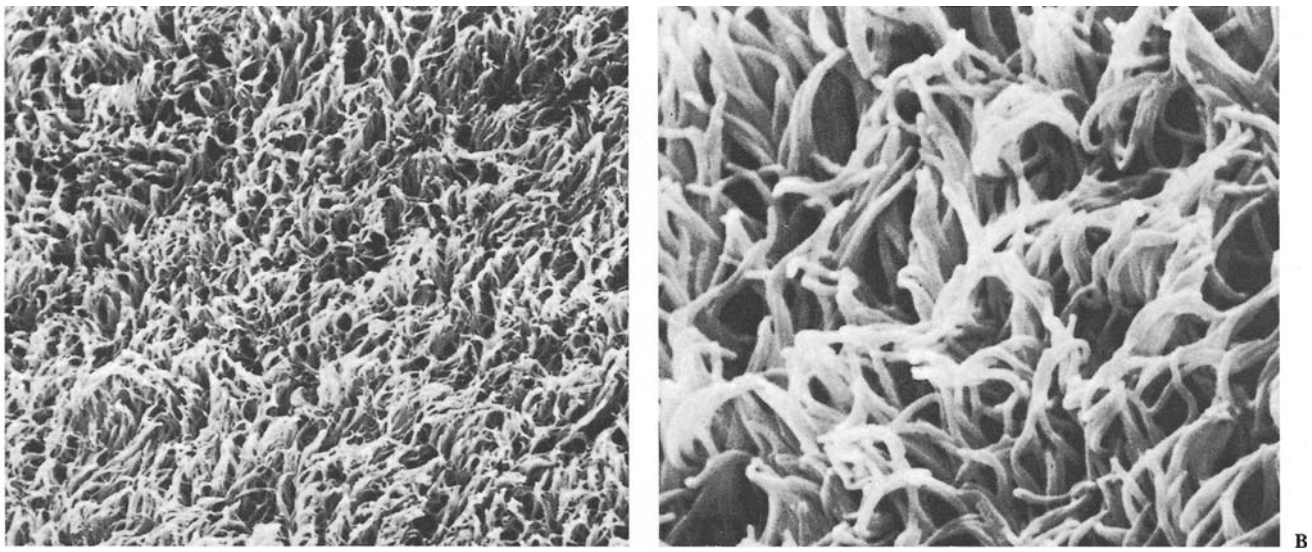

FIGURE 2.10. By scanning electron microscopy (SEM), cilia completely carpet the luminal surface of large airways. The presence of nonciliated cells is not appreciated from the surface. **A.** Swine, ×2500. **B.** Swine, ×11,000. (Prepared by Dr. N.-S. Wang.)

common and varied; these include compound or fused cilia, deranged axonemes with supernumerary or missing microtubules, internalized (cytoplasmic) or shed cilia, and other defects. (For a further discussion of cilia defects, see Chapter 5.)

Goblet Cells

The goblet cell is the most common nonciliated cell, and it extends from the larger bronchi to the smaller bronchi but is absent in the bronchioles. The ratio of ciliated to goblet cells is estimated to be between 7:1 and 25:1 in the large bronchi (Figs. 2.9 and 2.12).

The goblet cell has a basal nucleus, a well-developed rough endoplasmic reticulum, a Golgi apparatus, and abundant apical collections of mucous granules forming a "goblet" appearance (Fig. 2.13). The mucous granules are released into the bronchial lumen by the fusion and then the fenestration of the membranes of the granule and the cell, representing merocrine-type secretion. In excessive production and release, such as is seen in status asthmaticus, the apical portion of a goblet cell may appear to be completely replaced by an amorphous mass of mucus that extends in continuity from the cell into the mucous layer. Mucus in the lung, presumably like that in the intestine, is secreted for protection. It consists of acidic glycosaminoglycans, though the composition may vary during pathologic conditions. Goblet cells can divide mitotically and may increase in number drastically in any acute bronchial irritation, replacing almost all ciliated cells within 2 to 3 days. The recovery of ciliated cells is equally fast, and in chronic irritations certain balances develop between the two processes. Excessive goblet cell hyperplasia may disrupt the continuity of ciliary flow, and an excessive amount of mucus may obliterate the air passage, especially in small scarred airways. Although goblet cells contribute to the gel layer of bronchial mucus, the major source of mucus is the submucosal gland.

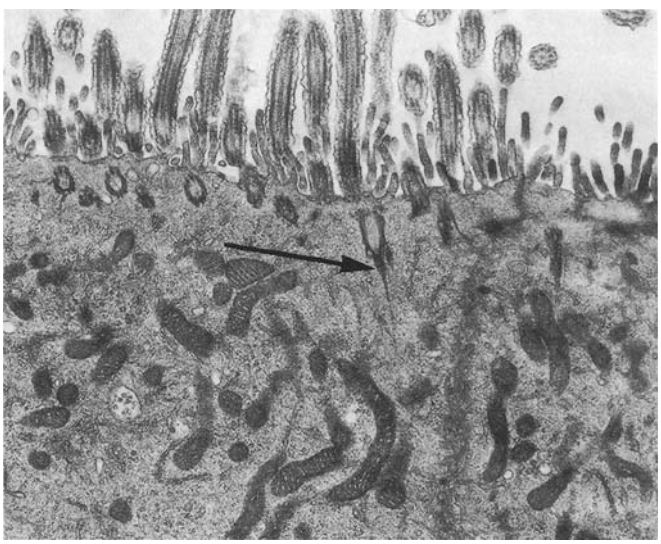

FIGURE 2.11. Mitochondria accumulate adjacent to cilia in ciliated cell. Long striated root (arrow) extends deeply from basal body of cilia. Human. Transmission electron microscopy (TEM) ×11,000. (Prepared by Dr. N.-S. Wang.)

Basal Cells

All ciliated and nonciliated cells in the bronchial mucosa are derived from the basal cell. The basal cell of the

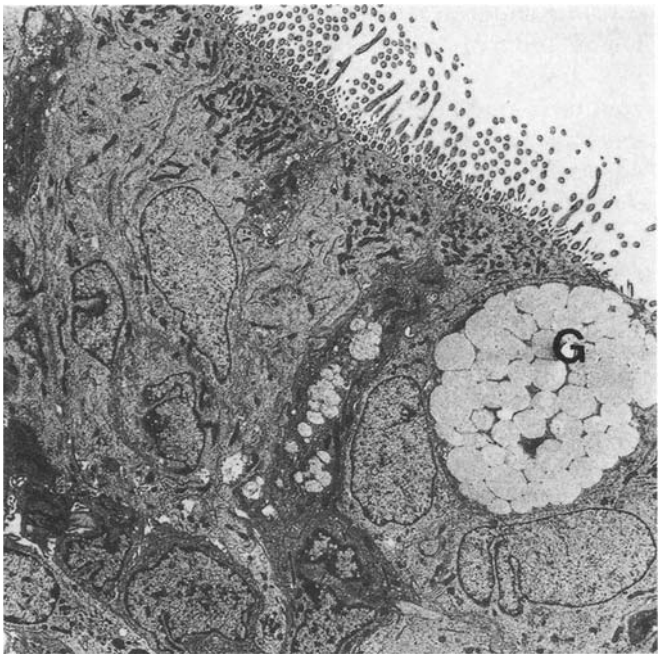

FIGURE 2.12. Ciliated cell is the most common cell type in bronchial mucosa. Large goblet cell (G) appears pale. Darkly stained basal cell at bottom of mucosa is smaller than other tall columnar cells. Human. TEM, ×2500. (Prepared by Dr. N.-S. Wang.)

bronchus is a pluripotential reserve cell that has a light and electron microscopic appearance similar to that of the epidermis. This cell is triangular with one of the broader sides firmly anchored on the basement membrane by hemidesmosomes (Fig. 2.12). The nucleus is large, and the organelles are scanty in the cytoplasm, which contains mainly loosely scattered ribosome complexes and tonofilaments. Desmosome complexes are prominent between cells.

Unlike the rest of the bronchial epithelium, the basal cell usually survives mucosal injuries to ensure a complete reconstruction of the bronchial mucosa. Prolonged irritation stimulates the proliferation of the basal cells (basal cell or reserve cell hyperplasia) or induces their differentiation into one or more differentiated forms. Deranged or mixed forms, which contain organelles of different types of cells, are also common, especially in the dysplastic and neoplastic epithelium that arise out of these cells (Fig. 2.14).

The Dense Core (Neuroendocrine) Cell and Neuroepithelial Bodies

See Chapter 36, Neuroendocrine Carcinomas, for a detailed discussion of neuroendocrine cells.

Other Bronchial Lining Cells

Brush cells, also termed tuft, caveolated, multivesicular, and fibrillovesicular cells, are a special type of cell characterized by blunt microvilli and having disk- or rod-like inclusions of unknown functions. These cells have been identified from the nose to the alveoli in many species, but have not been found in humans except under certain disease states.[26] The function of the pulmonary brush cell is obscure.

Bronchioles

A bronchus becomes a membranous bronchiole when cartilage completely disappears from its wall (Fig. 2.15). This occurs when the diameter of the airway decreases to about 1 mm. The terminal membranous bronchiole leads into the acinus, the functional unit of the lung, which consists of the respiratory bronchiole, alveolar ducts, alveolar sac, and alveoli (see below). The lung has approximately 30,000 terminal bronchioles, and each drains and concentrates the contents of approximately 10,000 alveoli.

Membranous bronchioles (including the terminal bronchiole) are lined completely by epithelial cells. This epithelium consists of ciliated columnar cells and nonciliated Clara cells. These bronchioles derive their mechanical support from the tethering effect exerted by the attached elastic fibers of the surrounding alveoli. Alveolar elastic fibers connect to the adventitia of the small airways and

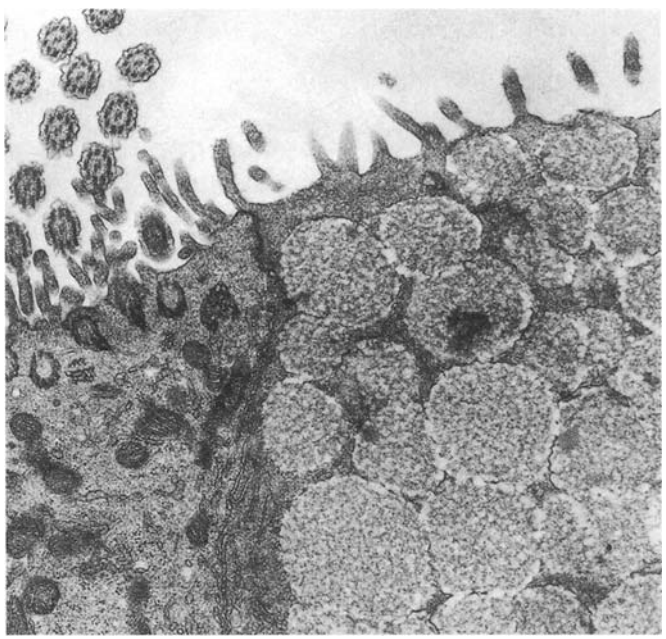

FIGURE 2.13. Multiple mucous granules accumulate near apex of goblet cell with amorphous and reticular appearance. Human. TEM, ×11,000. (Prepared by Dr. N.-S. Wang.)

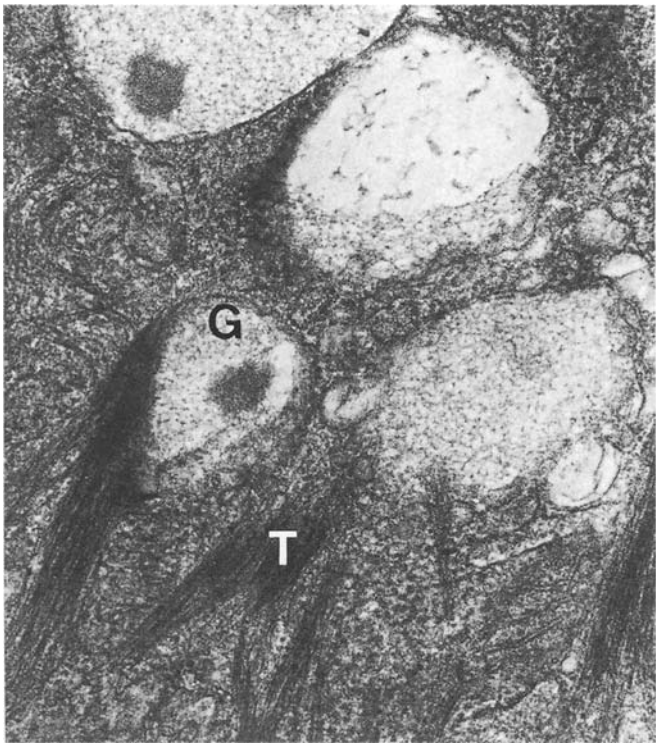

FIGURE 2.14. Mucous granules (G) and tonofilaments (T) are present within a dysplastic cell in bronchial mucosa. Human. TEM, ×38,000. (Prepared by Dr. N.-S. Wang.)

help prevent the collapse of the small airways during the final phase of expiration (Fig. 2.15A). Their destruction in lungs with emphysema causes a premature collapse of these small airways and obstruction of the airflow (see Chapter 24).

The terminal bronchiole gives rise to the respiratory bronchiole, in which alveoli are present in the bronchiolar wall (Fig. 2.16). Usually there are three generations of respiratory bronchioles, although some variation between one and five generations is possible. Ciliated cells extend to the bronchioloalveolar junction. In these more peripheral locations, they are short and decreased in number but maintain the continuity of the ciliary flow by a network arrangement around the nonciliated Clara cells (see below). This transitional zone is generally believed to be a normal lung structure, and formation of new alveoli in the small bronchioles is a normal process during the postnatal growth period, extending from birth until about 10 years of age. Direct epithelial-lined channels between membranous bronchioles and adjacent alveoli have been termed canals of Lambert (Fig. 2.15C). Depressions and eventual fistulous perforations of the wall of small membranous bronchioles also commonly occur in lung damage, especially in small-airway injury associated with tobacco use, leading to peribronchiolar proliferation and exten-

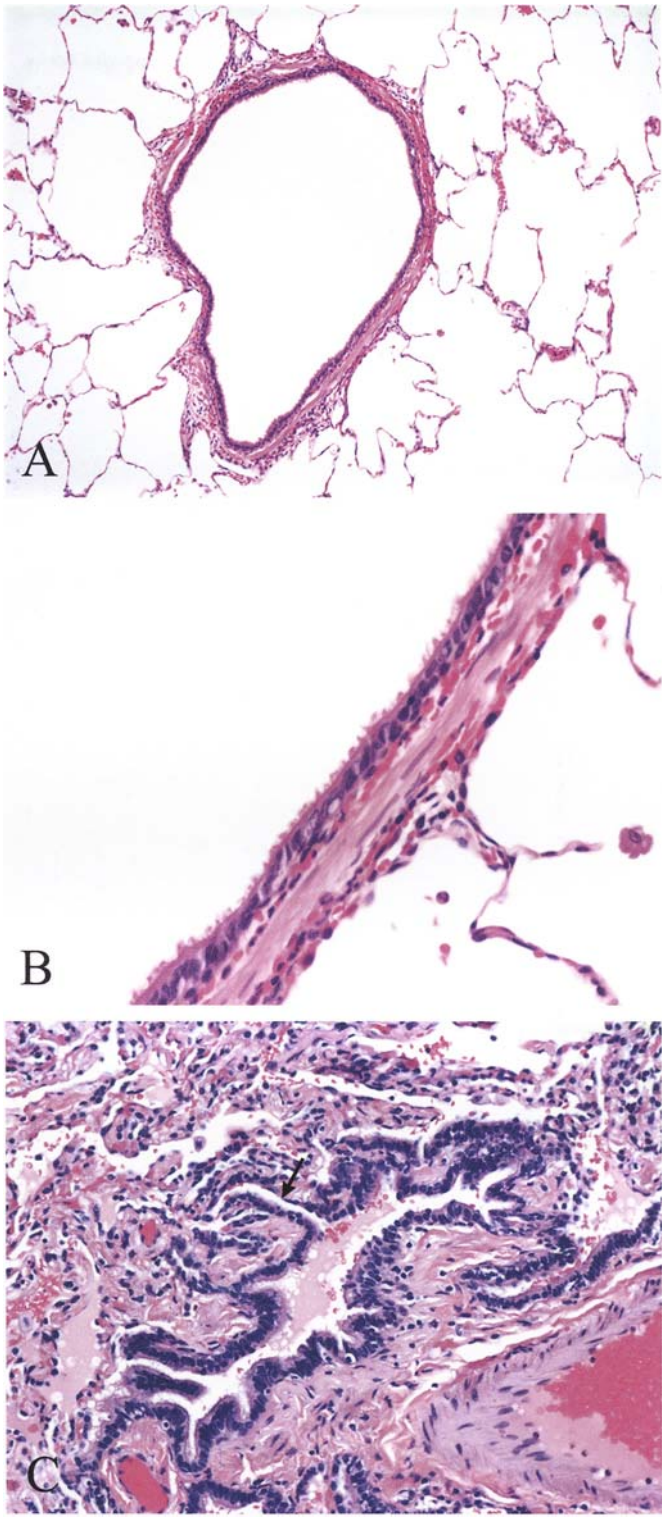

FIGURE 2.15. **A.** Membranous bronchiole with alveolar attachments. **B.** Wall of membranous bronchiole. Note single cell layer of ciliated epithelium and narrow fascicles of smooth muscle. **C.** Canal of Lambert. Narrow epithelial-lined channel (arrow) extends directly into adjacent lung parenchyma from a small membranous bronchiole.

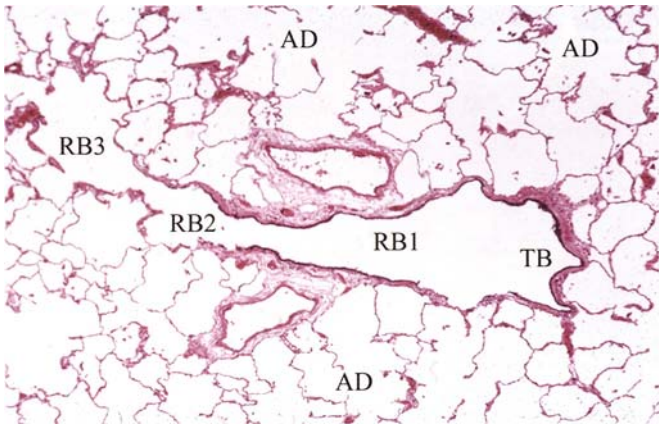

FIGURE 2.16. Respiratory bronchiole and alveolar ducts. TB, terminal bronchiole; RB1, 2, and 3, three orders of respiratory bronchiole; AD, representative alveolar ducts.

sion of bronchiolar lining cells into the alveolar region ("Lambertosis").

Clara Cells

The Clara cell is a nonciliated cuboidal cell found in both the membranous and respiratory bronchioles that replaces the disappearing goblet cell in small bronchioles. The Clara cell has an apical surface that bulges into the lumen, is rich in endoplasmic reticulum and mitochondria, and contains a prominent Golgi apparatus with apically located secretory granules that stain positively with periodic acid-Schiff (PAS)-diastase (Fig. 2.17). The Clara cells have been shown to secrete surfactant apoprotein that serves to decrease the surface tension in this area of the lung and keep these small channels open.[27] The Clara cell also serves as the reserve and reparatory cell in the small airways, a role similar to the basal cell more proximally and the alveolar type II cell more distally.[28]

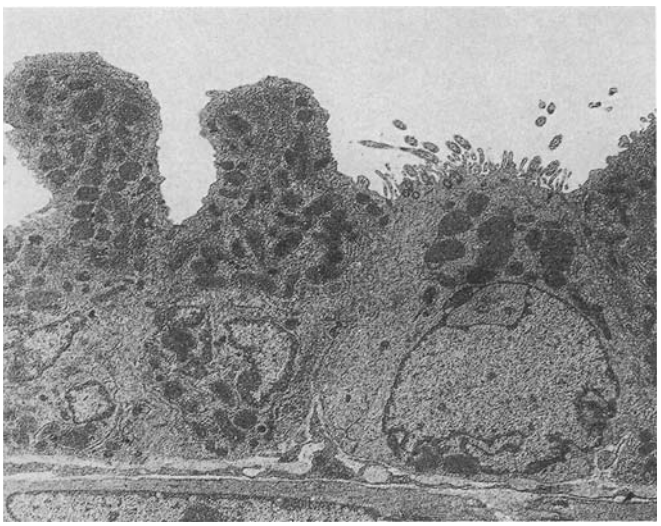

FIGURE 2.17. Electron micrograph of a Clara cell. Clara cells are taller than ciliated cells in small bronchioles. Note flame-shaped cytoplasmic processes rich in mitochondria, endoplasmic reticulum, and secretory granules. Mouse. TEM, ×4500. (From Wang NS, Huang SN, Sheldon H, Thurlbeck WM. Ultrastructural changes of Clara and type II alveolar cells in adrenalin-induced pulmonary edema in mice. Am J Pathol 1971;62:237–252, with permission from the American Society for Investigative Pathology.)

Parenchyma

Anatomic Subunits

Lobules

The secondary lobule of Miller is the smallest unit delineated by fibrous septa in the lung, and the smallest macroscopically observed unit of lung parenchyma.[29] Each lobule measures from 1 to 2.5 cm in maximal dimension and contains three to five acini (see below) (Fig. 2.18).[6,30] In adult lungs the lobule is best observed in the peripheral subpleural areas where interlobular septa extend from the visceral pleura, incompletely demarcating polyhedral units of lung parenchyma (Fig. 2.18A). Lobular architecture is much better defined in fetal or young children's lungs, especially in the upper lobe (Fig. 2.18B). The boundaries of the lobules are also readily recognized on the surface of the visceral pleura as the hexagonal pattern of lymphatic distribution (Fig. 2.1). Well-defined lobules are obscure in the central regions of normal adult lungs because the continued postnatal proliferation of alveoli stretches and disrupts the continuity of the interlobular septa.[12] Airways and pulmonary arteries enter the central portion of the lobule while pulmonary veins transport blood in the interlobular septa (Fig. 2.18C). The lobule is an important unit in chest radiology and histopathology, and some diseases such as emphysema are classified by their intralobular distribution of lesions (see Chapter 24). Interlobular septa are widened and accentuated in pulmonary edema and are visualized radiographically as Kerley B lines (see Fig. 28.42 in Chapter 28). With the advent of high-resolution chest computed tomography (CT) scans, the secondary lobule has assumed even greater importance in the recognition of radiographic patterns of lung disease.[2,31,32]

The primary lobule of Miller, which refers to the distal portion of the acinus, originates from the last-order respiratory bronchiole and includes the divisions of the alveolar ducts, alveolar sacs, and attached alveoli (Fig. 2.19A). The primary lobule has been superseded by the acinus as the practical basic unit of lung anatomy (see below).[6,30,32]

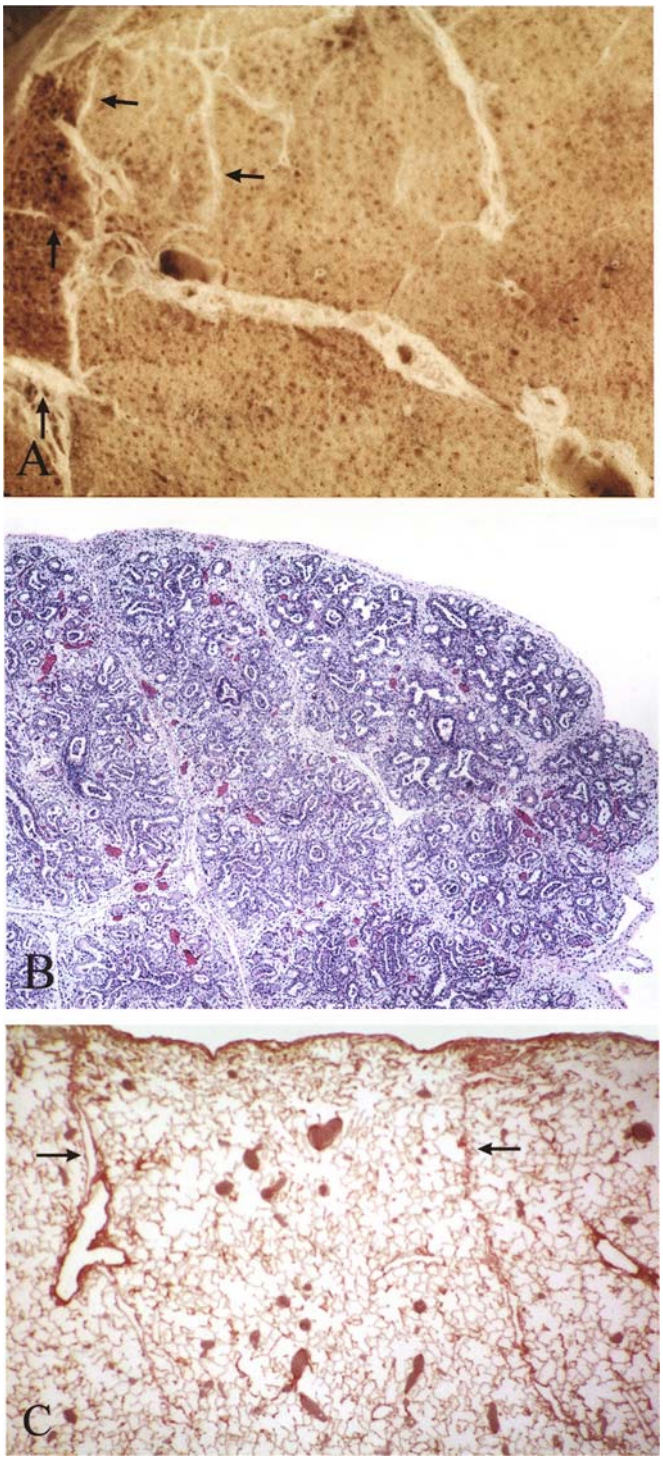

FIGURE 2.18. **A.** Macroscopic view of lung parenchyma showing interlobular septa (arrows) demarcating secondary lobules. The visceral pleura is in the left upper corner (barium sulfate impregnation). **B.** Secondary lobules are prominently visualized in the lung of a 21-week gestational age fetus. **C.** Microscopic view of secondary lobules in an adult lung following pulmonary arterial injection of barium–gelatin contrast media. Interlobular septa are demarcated with arrows. Note filling of arteries in the centrilobular zone while veins are empty. Visceral pleura is at top. (EVG.)

Acinus

The pulmonary acinus is the unit of lung distal to the last conducting airway, the terminal bronchiole (Fig. 2.19).[29,30] In lung casts, the acinus measures approximately 7.5 × 8.5 mm and consists of about three divisions of respiratory bronchioles and several divisions of alveolar ducts, terminating in alveolar sacs with their grape-like clusters of alveoli.[1,29] In adults the number of alveoli within the acinus ranges from 1500 to 4000 alveoli.[32] Acini have no septal boundaries, thus allowing for collateral ventilation, and they are not visible as defined units either grossly or microscopically (Fig. 2.19B). However, they have been delineated by means of corrosion casts.[29,32] Historically the acinus has been important histopathologically in defining the intraparenchymal spread of tuberculous lesions, and in the classification of emphysema into centriacinar and panacinar variants.[32] By virtue of the localization of bronchioles in the central portion of the lobule, the terms *panacinar* and *centriacinar* are synonymous with panlobular and centrilobular, respectively (see Chapter 24).[32]

Alveoli

Where alveoli completely replace the bronchiolar epithelial cells, the air passage, known as the alveolar duct, terminates in a semicircular blind end called the alveolar sac, which is surrounded by four or more alveoli.

The distal portion of the lung is formed by multifaceted and cup-shaped compartments called alveoli that have diameters of 150 to 500 µm (average, 250 µm) (Fig. 2.20). In a 70-kg man, there are about 300 million alveoli with a gas-exchanging alveolar surface of approximately 143 m^2 contained within an average lung volume of 4.3 L. After the age of 30 or 40 years the lungs undergo a progressive dilatation of air spaces. Alveolar ducts enlarge while adjacent alveoli appear flattened (alveolar duct ectasia), although it is uncertain whether or not there is actual destruction of alveolar septa. It has been recommended that the term *aging lung* be used rather than the traditional term *senile emphysema* for aging-associated changes.[33]

The orifices of alveoli along the alveolar ducts and alveolar sacs are formed by thick elastic and collagen bundles that are the continuum of bronchial and bronchiolar elastic bundles (Fig. 2.20B). From the orifice bundle, finer elastic fibers spread out further, resembling a basket, and are interwoven with capillaries. This network of elastic fibers and capillaries is plated (like wallpaper) on both sides by thin layers of type I alveolar lining cells. All elastic fibers, including the fine meshwork of the alveolus, are interconnected in all directions to form an integrated elastic network that is fundamental to the